

*Successes and Challenges in Modeling Wave-Plasma  
Interactions in Magnetically Confined Plasmas*

Cynthia K. Phillips  
PPPL

# Participants in the Center for Simulation of Wave-Plasma Interactions

L.A. Berry, D.B. Batchelor, D. L. Green,  
**E. D`Azevedo**, E. F. Jaeger



D. Smithe T. Austin, J. Carlsson



R.W. Harvey, A.P. Smirnov, Y. Petrov  
**CompX**

D. D'Ippolito, J. Myra - ***Lodestar Research***

M. Choi The logo for General Atomics features a stylized four-pointed star or diamond shape to the left of the word "GENERAL ATOMICS" in a bold, white, sans-serif font.

P.T. Bonoli, J.C. Wright,  
H. Kohno<sup>#</sup>, A. Bader<sup>\*</sup>



**C.K. Phillips, E. Valeo, N. Bertelli**



M. Brambilla The logo for the Max-Planck-Institut für Plasmaphysik (IPP) features the letters "IPP" in a white, sans-serif font, set against a solid blue square.

R. Maggiora  
***Politecnico di Torino***

# Experimental Observations and ITER provide the motivation for the computational modeling

J.C. Hosea, R. Ellis, B. LeBlanc,  
R. Perkins, G. Taylor, J.R. Wilson



P.M. Ryan, J. W. Wilgen



S. Wukitch, G. Wallace, M. Porkolab,  
Y. Lin, R. Parker, S. Shiraiwa plus  
many graduate students

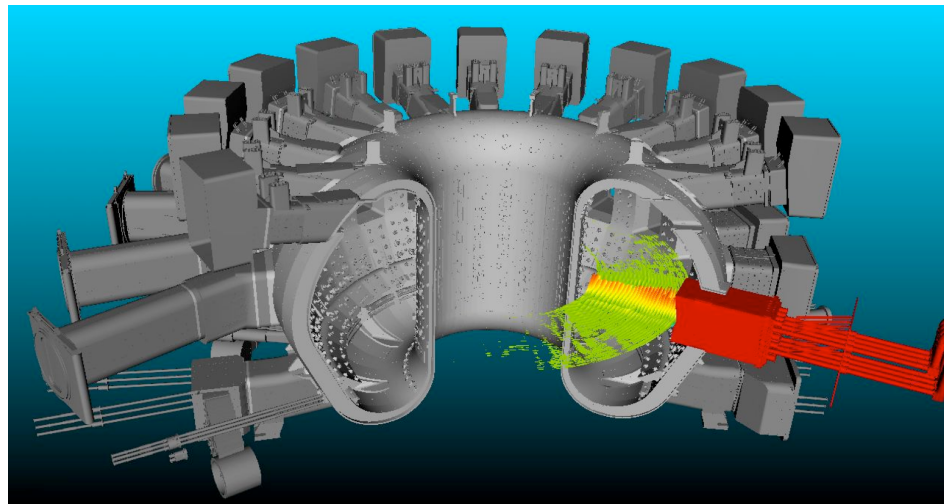


R. Pinsker, T. Luce, C. Petty,  
R. Prater, V. Chan

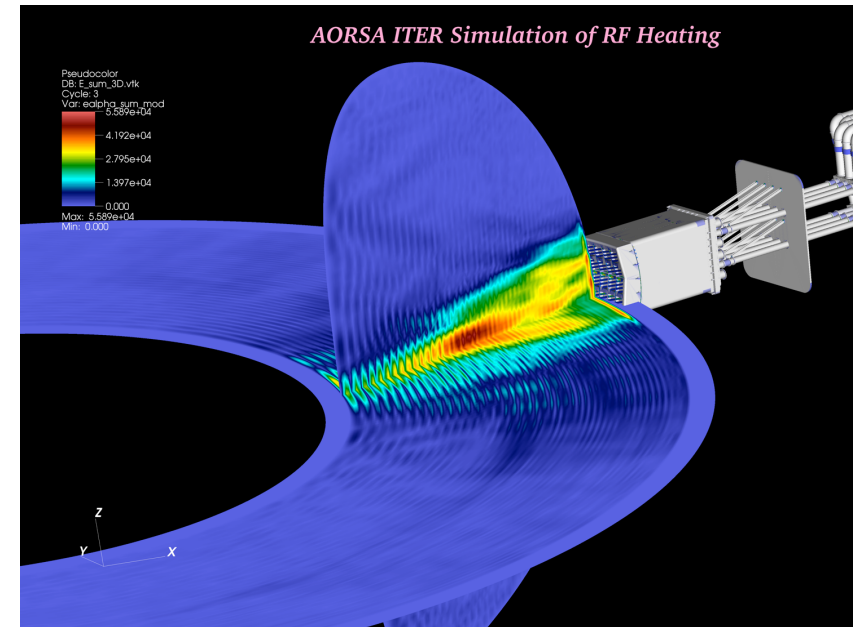


# Radio Frequency Waves will be applied to ITER to achieve “burning plasma” conditions

E.F. Jaeger *et al* ORNL



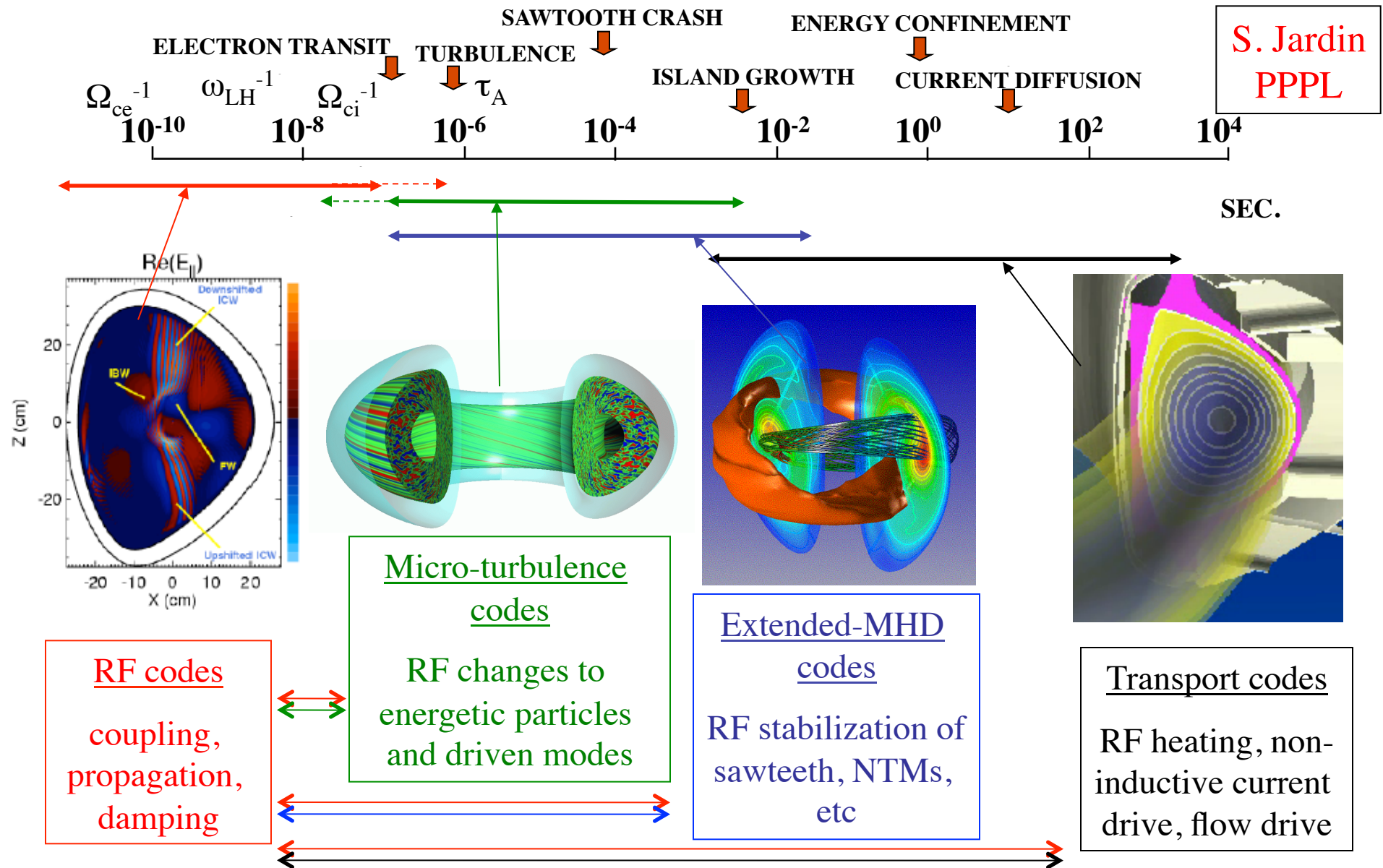
*Visualization of the 3-D wave fields in the equatorial plane of ITER showing the vacuum vessel and RF antenna structure (red).*



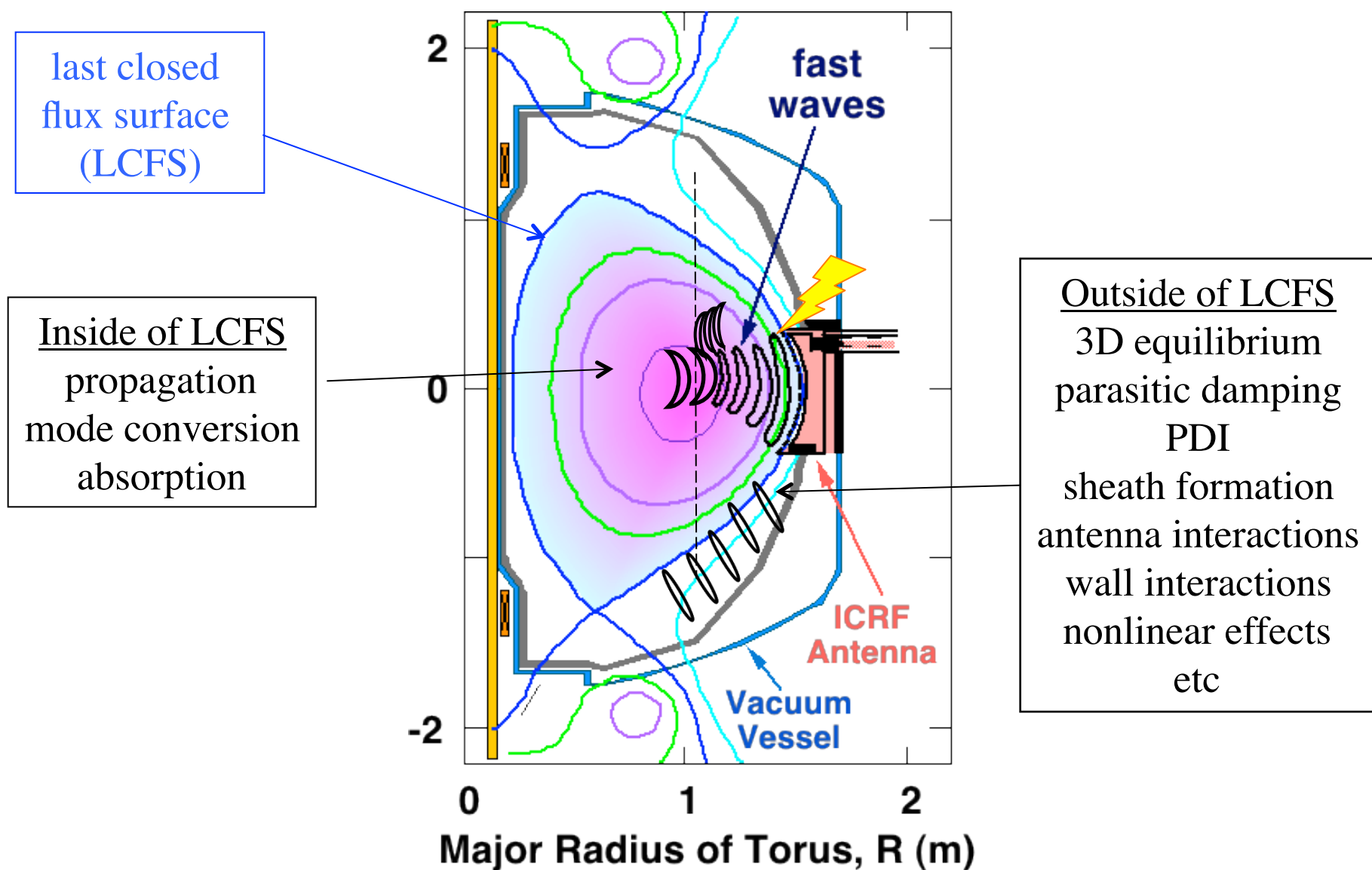
*Visualization of the 3-D wave fields in poloidal and equatorial planes in front of the ITER RF antenna (~2 m high).*

Ohmic heating insufficient since  $P \sim E \cdot j \sim \eta j^2 \sim T_e^{-3/2} \rightarrow 0$  as electron temperature increases  $\rightarrow$  need auxiliary heating

# RF wave-plasma interactions important on multiple timescales in fusion plasmas



# A wide range of spatial scales arise in wave propagation, absorption and coupling to the plasma

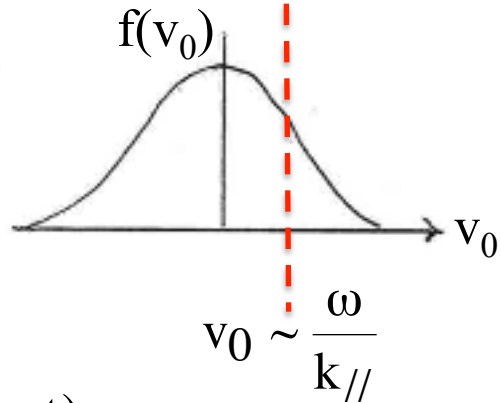


# Outline of Presentation

- Model equations and assumptions
- Challenges in resolving rf field structures with widely disparate spatial scales
  - mode conversion in the Ion Cyclotron Range of Frequencies (ICRF) regime on Alcator C-Mod
  - possible mode conversion in the High Harmonic Fast Wave (HHFW) regime on NSTX
- Challenges in self-consistently including rf modifications of the plasma equilibrium on time scales longer than the fast “rf time scales”
  - ICRF regime on C-Mod
  - HHFW with Neutral Beam Injection (NBI) on NSTX
- Challenges and Approaches to “core to edge” simulations
  - Fields in edge regions near the antenna and vessel
  - Connections to fields in core
- The Frontier?
- Closing remarks

# Dynamics of wave-particle interactions motivates use of spectral methods

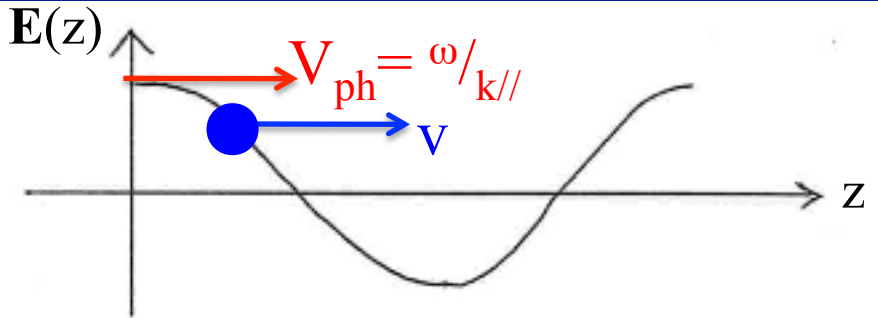
Landau damping – parallel dynamics:



$$\vec{E} = \hat{z}E_1 \cos(kz - \omega t)$$

$$m \frac{dv}{dt} = qE_1 \cos(kz - \omega t) \quad v = v_0 + v_1 + v_2 + \dots$$

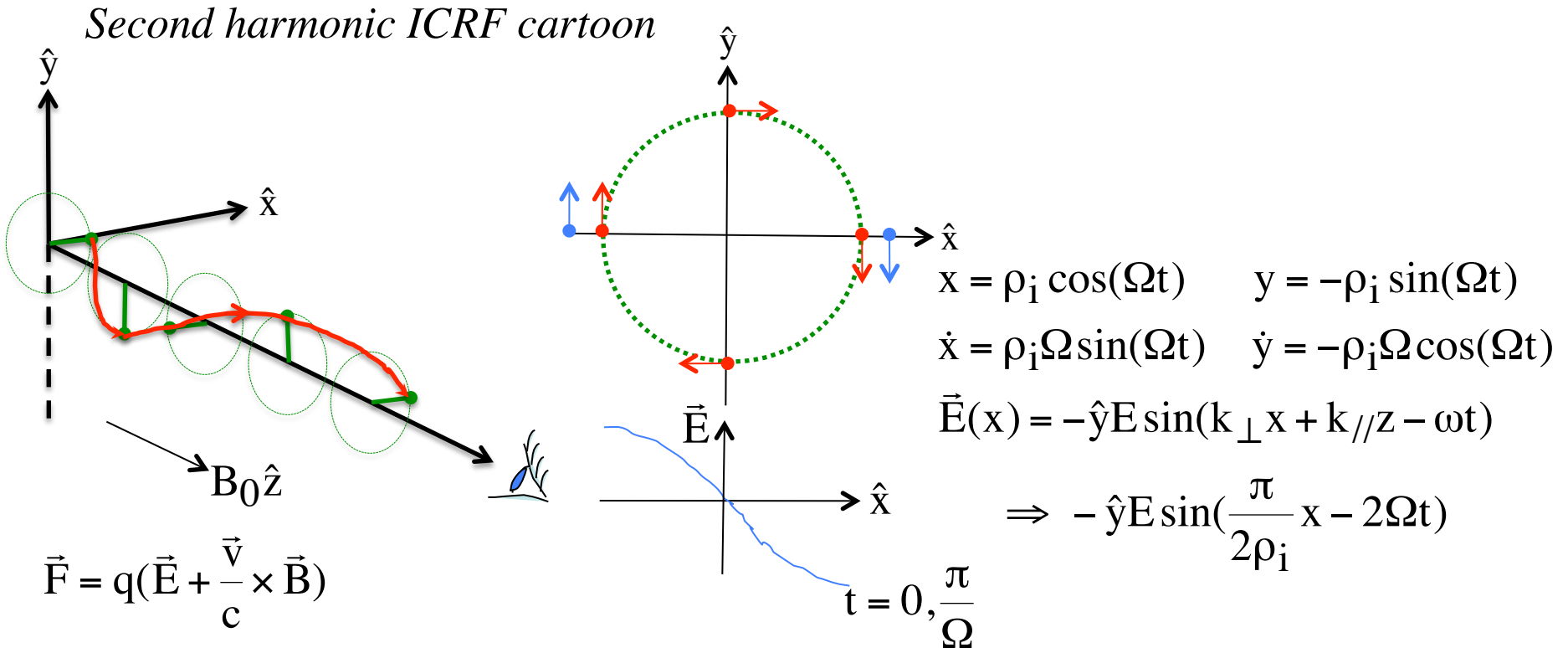
$$\left\langle \frac{d}{dt} \frac{1}{2} mv^2 \right\rangle_{z_0, f(v_0)} = \left\langle mv_1 \frac{dv_1}{dt} + mv_0 \frac{dv_2}{dt} \right\rangle_{z_0, f(v_0)} \rightarrow -\frac{\pi \omega q^2 E_1^2}{2mk|k|} \left[ \frac{df(v_0)}{dv} \right]_{v_0 = \frac{\omega}{k}}$$



particles moving with  $v \sim V_{ph} = \omega / k_{\parallel}$   
can gain or lose energy

⇒ parallel wave vector (and equilibrium distribution) determine wave absorption (or growth)

# Cyclotron resonances depend on $k_{\perp}$ as well as $k_{\parallel}$



$$\left\langle \frac{d}{dt} W_{\perp} \right\rangle_t = \left\langle \vec{v} \cdot m \frac{d\vec{v}}{dt} \right\rangle_t \sim \left\langle q [-E \sin(k_{\perp} \rho_i \cos(\Omega t + \phi))] [-\rho_i \cos(\Omega t + \phi)] \right\rangle_t$$

$$\neq 0 \quad \text{provided} \quad \omega = (n \pm 1)\Omega$$

**In principle, RF wave physics across many time scales could be explored by direct time and space solutions of the coupled Boltzman and Maxwell equations**

$$\left( \frac{\partial f}{\partial t} + \bar{v} \cdot \frac{\partial f}{\partial \vec{r}} + \frac{q}{m} \left[ \vec{E} + \frac{\vec{v} \times \vec{B}}{c} \right] \cdot \frac{\partial f}{\partial \vec{v}} = \frac{\partial f}{\partial t} \Big|_{\text{coll}} \right)_s$$

$$\nabla \times \vec{E} = -\frac{1}{c} \frac{\partial \vec{B}}{\partial t} \quad \nabla \times \vec{B} = \frac{4\pi}{c} [\vec{J}_p + \vec{J}_{\text{ant}}] + \frac{1}{c} \frac{\partial \vec{E}}{\partial t}$$

$$\nabla \cdot \vec{E} = 4\pi\rho \quad \nabla \cdot \vec{B} = 0$$

$$\rho = \sum_s q_s \int f_s d^3 v \quad \vec{J}_p = \sum_s q_s \int \vec{v} f_s d^3 v$$

plus boundary conditions at vessel wall

[note: fields have been averaged over the Debye sphere]

*.....but this is beyond our current capabilities*

*(except possibly for studies of nonlinear phenomena in edge, like sheath, PDI, etc with PIC codes)*

## In practice, the equations are solved self-consistently on the fast rf and somewhat longer quasilinear time scales

For time harmonic (rapidly oscillating) wave fields  $\mathbf{E}$  with frequency  $\omega$ , Maxwell's equations reduce to the Helmholtz wave equation:

$$-\nabla \times \nabla \times \mathbf{E} + \frac{\omega^2}{c^2} \left( \mathbf{E} + \frac{4\pi i}{\omega} \mathbf{J}_p \right) = -\frac{4\pi i \omega}{c^2} \mathbf{J}_{\text{ant}}$$

The plasma current ( $\mathbf{J}_p$ ) is a non-local, integral operator (and non-linear) on the rf electric field and conductivity kernel:

$$\mathbf{J}_p(\mathbf{r}, t) = \sum_s \int d\mathbf{r}' \int_{-\infty}^t dt' \sigma(f_{0,s}(E), \mathbf{r}, \mathbf{r}', t, t') \mathbf{E}(\mathbf{r}', t')$$

The long time scale response of the plasma distribution function is obtained from the bounce averaged Fokker-Planck equation:

$$\frac{\partial}{\partial t} (\lambda f_0) = \nabla_{\mathbf{u}_0} \cdot \Gamma_{\mathbf{u}_0} + \langle\langle S \rangle\rangle + \langle\langle R \rangle\rangle^0 \quad \text{where} \quad \nabla_{\mathbf{u}} \cdot \Gamma_{\mathbf{u}} = C(f_0) + Q(\mathbf{E}, f_0)$$

**Wave Solvers**  
**(AORSA)**  
**(TORIC)**

**Plasma Response**  
**(CQL3D)**



*Need to solve this nonlinear, integral set of equations for wave fields and velocity distribution function self-consistently. This requires an iterative process to attain self-consistency.*

# On the “rf” time scale, the Vlasov-Maxwell equations are linearized and solved in the frequency domain

Assume localized resonant interactions and known locally homogeneous plasma profiles

$$\vec{E} = \vec{E}_1 \quad \vec{B} = B_0 \hat{z} + \vec{B}_1 \quad \text{plus Maxwell Equations}$$

$$\frac{\partial f_1}{\partial t} + \vec{v} \cdot \frac{\partial f_1}{\partial \vec{r}} + \frac{q}{mc} [\vec{v} \times \vec{B}_0] \cdot \frac{\partial f_1}{\partial \vec{v}} = -\frac{q}{m} \left[ \vec{E}_1 + \frac{\vec{v}}{c} \times \vec{B}_1 \right] \cdot \frac{\partial f_0}{\partial \vec{v}} \quad \text{with } f_0 = f_0(v_{\perp}, v_{\parallel})$$

Solve using method of characteristics  $\Rightarrow$  integrate over unperturbed orbits, using Landau contours to satisfy causality

$$f_1(\vec{r}, \vec{v}, t) = -\frac{q}{m} \int_{-\infty}^t dt' e^{-i\omega t'} \vec{E}(\vec{r}'(t', \omega)) \cdot \left[ \vec{l}(1 - \frac{\vec{v}' \cdot \vec{k}}{\omega}) + \frac{\vec{v}' \vec{k}}{\omega} \right] \cdot \frac{\partial f_0}{\partial \vec{v}'}$$

Leading to the wave equation:

$$\nabla \times \nabla \times \vec{E}(\vec{r}, \omega) - \frac{\omega^2}{c^2} \left[ \vec{E}(\vec{r}, \omega) + \frac{4\pi i}{\omega} \vec{J}_p(\vec{r}, \omega) \right] = \frac{4\pi i}{\omega} \vec{J}_A(\vec{r}, \omega)$$

$$\vec{J}_p(\vec{r}, \omega) = \int d\vec{r}' \vec{\sigma}(\vec{r}, \vec{r}', \omega) \cdot \vec{E}(\vec{r}', \omega)$$

*Still very complicated!*

# The hot-plasma dielectric response is complicated..... even for infinite-homogeneous Maxwellian plasmas!

$$J_{p,s}(k, \omega) \rightarrow -i\omega/4\pi [ \chi_s(k, \omega) \cdot E(k, \omega) ] \quad (s \text{ is species index})$$

$$\chi_s = \left[ \hat{\mathbf{e}}_{\parallel} \hat{\mathbf{e}}_{\parallel} \frac{2\omega_p^2}{\omega k_{\parallel} w_1^2} \langle v_{\parallel} \rangle + \frac{\omega_p^2}{\omega} \sum_{n=-\infty}^{\infty} e^{-\lambda} \mathbf{Y}_n(\lambda) \right]_s,$$

$$\mathbf{Y}_n(\lambda) =$$

$$\begin{pmatrix} \frac{n^2 I_n}{\lambda} A_n & -in(I_n - I'_n)A_n & \frac{k_{\perp}}{\Omega} \frac{nI_n}{\lambda} B_n \\ in(I_n - I'_n)A_n & \left( \frac{n^2}{\lambda} I_n + 2\lambda I_n - 2\lambda I'_n \right) A_n & \frac{ik_{\perp}}{\Omega} (I_n - I'_n)B_n \\ \frac{k_{\perp}}{\Omega} \frac{nI_n}{\lambda} B_n & -\frac{ik}{\Omega} (I_n - I'_n)B_n & \frac{2(\omega - n\Omega)}{k_{\parallel} w_1^2} I_n B_n \end{pmatrix}$$

Infinite sum of modified Bessel functions of argument  $\lambda = \frac{1}{2} k_{\perp}^2 \langle \rho_L^2 \rangle$

$$A_n = \frac{1}{\omega} \frac{T_{\perp} - T_{\parallel}}{T_{\parallel}} + \frac{1}{k_{\parallel} w_{\parallel}} \frac{(\omega - k_{\parallel} V - n\Omega)T_{\perp} + n\Omega T_{\parallel}}{\omega T_{\parallel}} Z_0,$$

$$B_n = \frac{1}{k_{\parallel}} \frac{(\omega - n\Omega)T_{\perp} - (k_{\parallel} V - n\Omega)T_{\parallel}}{\omega T_{\parallel}}$$

$$+ \frac{1}{k_{\parallel}} \frac{\omega - n\Omega}{k_{\parallel} w_{\parallel}} \frac{(\omega - k_{\parallel} V - n\Omega)T_{\perp} + n\Omega T_{\parallel}}{\omega T_{\parallel}} Z_0,$$

$$Z_0 = Z_0(\xi_n), \quad \xi_n = \frac{\omega - k_{\parallel} V - n\Omega}{k_{\parallel} w_{\parallel}},$$

$$\frac{dZ_0(\xi_n)}{d\xi_n} = -2[1 + \xi_n Z_0(\xi_n)].$$

Landau and Doppler-shifted cyclotron resonances appear here

# The “local” dielectric tensor in the wave equation includes velocity-space integrals of derivatives of $f_0(v_\perp, v_{\parallel})$

The hot plasma susceptibility (conductivity) tensor for species “s” in a homogeneous, magnetized plasma\* is given by:

$$\tilde{\chi}_s = \frac{4\pi i}{\omega} \tilde{\sigma} = \frac{\omega_{ps}^2}{\omega} \int_0^\infty 2\pi v_\perp dv_\perp \int_{-\infty}^\infty dv_{\parallel} \hat{z}\hat{z} \frac{v_{\parallel}^2}{\omega} \left( \frac{1}{v_{\parallel}} \frac{\partial f_0}{\partial v_{\parallel}} - \frac{1}{v_\perp} \frac{\partial f_0}{\partial v_\perp} \right)_s + \\ \frac{\omega_{ps}^2}{\omega} \int_0^\infty 2\pi v_\perp dv_\perp \int_{-\infty}^\infty dv_{\parallel} \sum_{n=-\infty}^{n=\infty} \left[ \frac{v_\perp U}{\omega - k_{\parallel} v_{\parallel} - n\Omega} \vec{T}_n \right]_s$$

where:

$$\vec{T}_n = \begin{bmatrix} \frac{n^2 J_n^2}{z^2} & \frac{i n J_n J'_n}{z} & \frac{n J_n^2 v_{\parallel}}{z v_\perp} \\ -\frac{i n J_n J'_n}{z} & (J'_n)^2 & -\frac{i n J_n J'_n v_{\parallel}}{v_\perp} \\ \frac{n J_n^2 v_{\parallel}}{z v_\perp} & \frac{i n J_n J'_n v_{\parallel}}{v_\perp} & \frac{J_n^2 v_{\parallel}^2}{v_\perp^2} \end{bmatrix} \quad U = \frac{\partial f_0}{\partial v_\perp} - \frac{k_{\parallel}}{\omega} \left[ v_\perp \frac{\partial f_0}{\partial v_{\parallel}} - v_{\parallel} \frac{\partial f_0}{\partial v_\perp} \right]$$

$$J_n = J_n \left( \frac{k_\perp v_\perp}{\Omega} \right)$$

and

$\vec{J}_{\text{plas}}(\vec{k}, \omega) = \frac{-i\omega}{4\pi} \sum_s \vec{\tilde{\chi}}(\vec{k}, \omega) \cdot \vec{E}(\vec{k}, \omega)$

\* Waves in Plasmas, T.H. Stix, [AIP, NY, 1992] Chapter 10

## Numerical evaluation of the velocity-space integrals in the dielectric tensor elements increases cpu time

- The velocity-space integrals are evaluated using the Plemelj formulas for integrals of the Cauchy form:

$$\lim_{v \rightarrow 0^+} \int_{-\infty}^{\infty} \frac{g(u)du}{u - iv - u_{//0}} = P \int_{-\infty}^{\infty} \left( \frac{g(u)du}{u - u_{//0}} \right) + i\pi \int_{-\infty}^{\infty} du g(u) \delta(u - u_{//0})$$

- The most expensive part of the computation is the evaluation of the Hermitian part of the dielectric tensor elements:

$$I = P \left( \int_{-\infty}^{\infty} du_{//} \frac{g(u_{//})}{u_{//} - u_{//0}} \right)$$

**normalized resonant parallel velocity**

- Time required to fill the matrix can be comparable to time required to invert the matrix for the wave fields*
- Distribution function may be generated by particle-based codes, so care must be taken to smooth those distributions carefully*

## “Full Wave” codes solve the wave equation in a numerically-specified tokamak equilibrium plasma

$$\nabla \times \nabla \times \vec{E} - \frac{\omega^2}{c^2} \vec{E} = \frac{4\pi i\omega}{c^2} [\vec{J}_{\text{ant}} + \vec{J}_p]$$

$$\text{where } \vec{J}_p(\vec{r}, \omega) = \int d\vec{r}' \tilde{\sigma}(\vec{r}, \vec{r}', \omega) \cdot E(\vec{r}', \omega) = \sum_s n_s q_s \vec{v}_s$$

“Full Wave” solution approach

- Solve for E-fields everywhere within some volume
- Superconducting boundary condition at metal walls
- Include highly simplified currents to model the antenna
- Use  $\sigma$  tensor with varying degrees of sophistication

Most “Full Wave” codes use spectral decomposition to represent the wave fields and to specify the  $\sigma$  tensor:

$$\Rightarrow \text{“easy” to identify } k_{\perp} \text{ and } k_{\parallel} \text{ when } \vec{B}_0 = \vec{B}_T(R)\hat{\phi} + \vec{B}_p(r)\hat{\theta}$$

**These codes must be run on multi-processor supercomputers to include sufficient modes in the expansions to achieve fine spatial resolution of short wavelength modes.**

## TORIC uses the finite Larmor radius (FLR) approximation to simplify the plasma dielectric tensor

- The Bessel functions are expanded for small argument and truncated at second-order in  $(k_{\perp}\rho)^2 \ll 1$  and terms  $\sim k_{\perp}$  are “inverse transformed”  $\sim \nabla_{\perp}$

$$J_n(z) = \sum_{m=0}^{\infty} \frac{(-1)^m}{m!(n+m)!} \left(\frac{z}{2}\right)^{n+2m} \quad \text{where } z = \frac{k_{\perp}v_{\perp}}{\Omega} \sim k_{\perp}\rho$$

- The resulting FLR wave equation contains only differential operators:

$$\nabla \times \nabla \times E - \frac{\omega^2}{c^2} \left[ E + \frac{4\pi i}{\omega} J^{(0)} + \frac{4\pi i}{\omega} J_{ion}^{(2)} + \frac{4\pi i}{\omega} J_{elec}^{(2)} \right] = \frac{4\pi i}{\omega} J^{(ant)}$$

(using the Smithe-Colestock-Kashuba model that ignores  $J^{(1)}$  terms)

- TORIC utilizes a poloidal mode expansion and radial finite elements in the poloidal plane and a Fourier decomposition in the toroidal direction.

$$E(\vec{r}) = \sum_{n_{\phi}} e^{in_{\phi}\phi} \sum_{m=-n \text{ mod } 2}^{n \text{ mod } 2} E_m(\psi, n_{\phi}) e^{im\theta}$$

and  $E_m(\psi, n_{\phi})$  is solved with nelm cubic Hermite polynomials

⇒ ***Results in a banded block tri-diagonal matrix with dense blocks to invert***

## AORSA solves the integral nonlocal wave equation, valid to “all orders” in $k_{\perp}\rho_i$

AORSA uses **collocation** to solve the “all orders” wave equation:

- Expand  $E$  and  $J_p$  in Fourier harmonics at  $n \times m$  points in space:

$$\vec{E}(x,y) = \sum_N e^{iN\phi} \sum_{n,m} \vec{E}_{N,n,m} e^{i(k_n x + k_m y)}$$

$$\vec{J}_p(x,y) = \sum_N e^{iN\phi} \sum_{n,m} \sigma(x,y, k_n, k_m) \cdot \vec{E}_{N,n,m} e^{i(k_n x + k_m y)}$$

- Solve the Fourier-expanded wave equation at each point in the  $n \times m$  space to find the  $n \times m$  Fourier coefficients

*Advantage:* most complete physics model, boundary conditions are easy, as is equilibrium geometry

*Disadvantage:* must invert a large, dense, full matrix

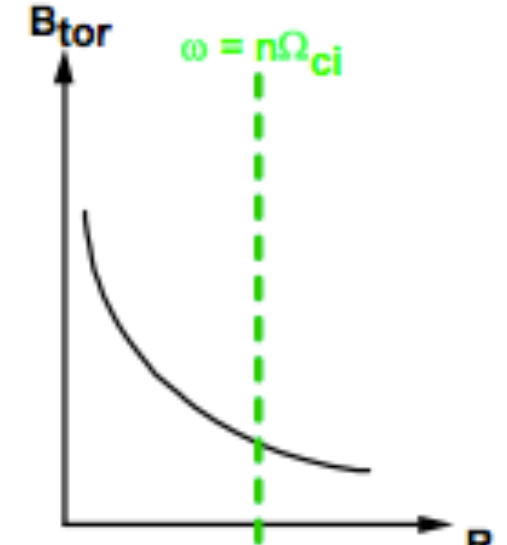
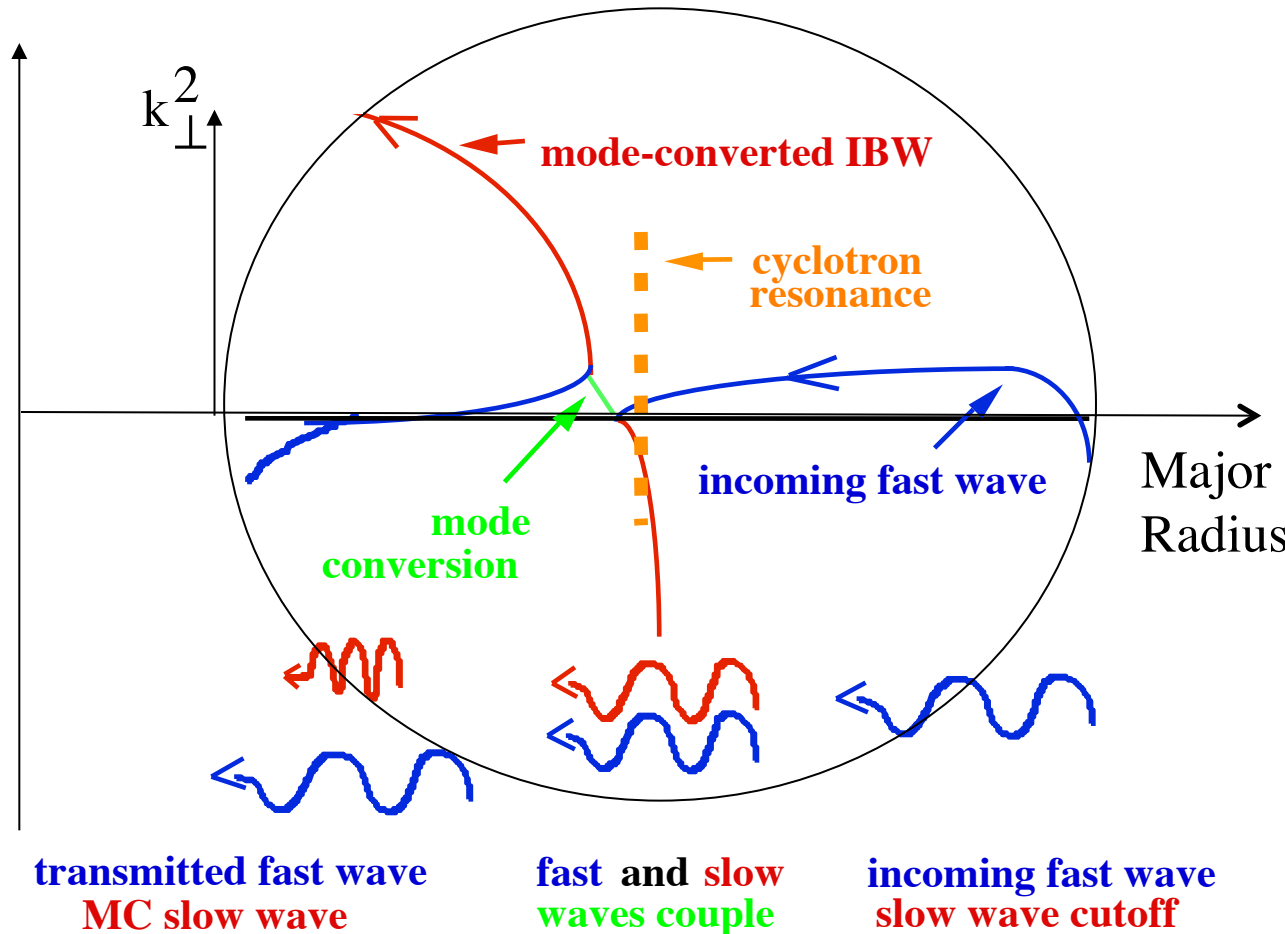
➡ can require lots of cpu time and many processors

*Spectral methods have been successful in simulating rf wave fields within the last closed flux surface, but:*

- Considerable cpu time is required for adequate resolution of wave structures, even in 2D tokamak cross sections
- CPU requirements for modeling waves in 3D devices, such as stellarators, is prohibitive
- Some discrepancies remain when comparing models against experimental measurements



# In some ICRF heating scenarios, mode conversion can occur when two waves co-exist locally



Recall:  $\vec{E} \sim \vec{E}_k e^{i(k_{\perp}r + k_{\parallel}z - \omega t)}$

## Mode conversion can be understood using a dispersion relation model for the waves

- assuming local homogeneity (WKB), large wavelengths relative to gyroradii (FLR -  $\rho / \lambda \ll 1$ ), and straight, uniform B field in z-direction, find dispersion relation:

$$a k_{\perp}^4 + b k_{\perp}^2 + c = 0$$

$$\vec{E} \sim \vec{E}(\vec{k}, \omega) e^{i(k_{\perp}x + k_{\parallel}z - \omega t)}$$

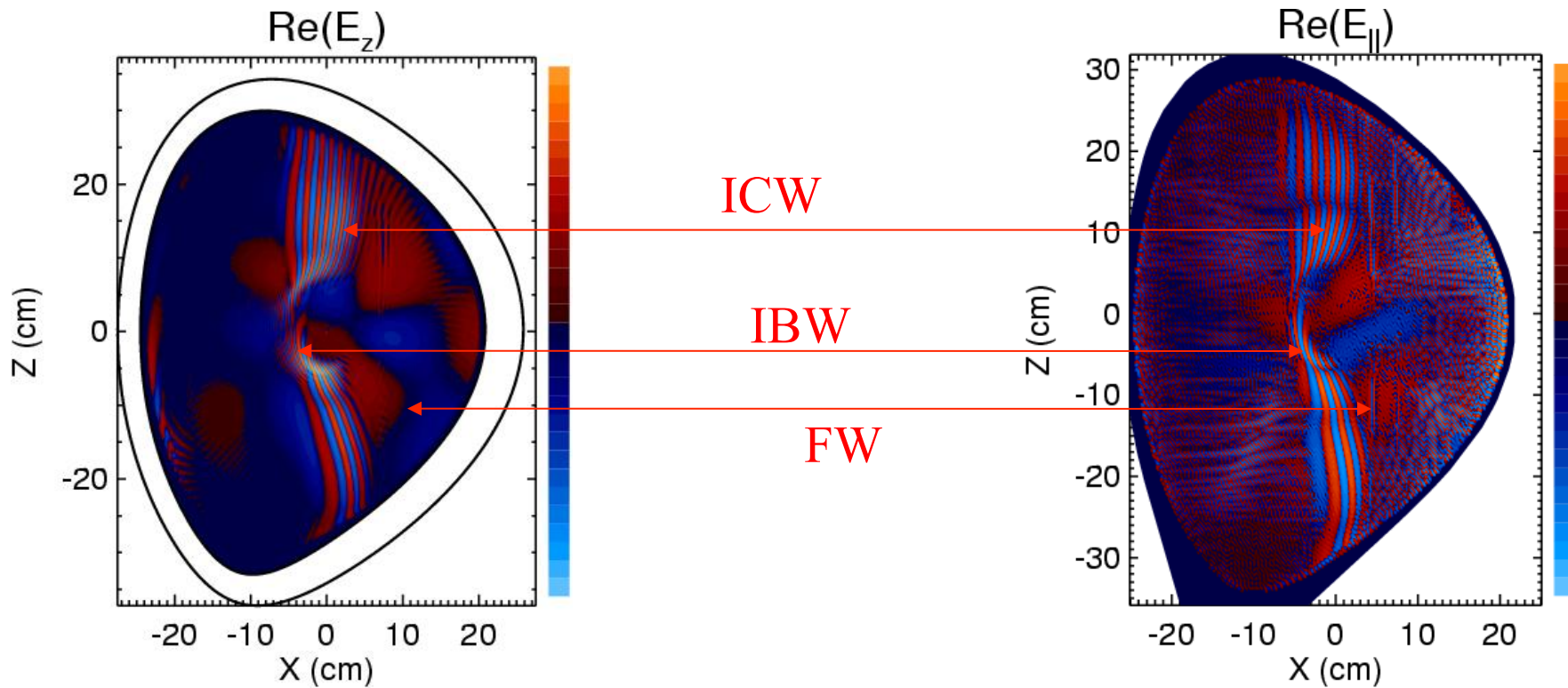
- If plasma varies in space, get localized absorption and/or mode conversion:

asymptotically  $k_{\perp, \text{slow}} \sim -b/a$  and  $k_{\perp, \text{fast}} \sim -c/b$

coupling occurs when  $b^2 - 4ac = 0$

- Away from the mode conversion layer, the slow wave is typically much shorter in wavelength than the fast wave*

## TORIC (FLR) and AORSA (all orders) found ion cyclotron wave (ICW) in addition to IBW and fast ICRFwaves



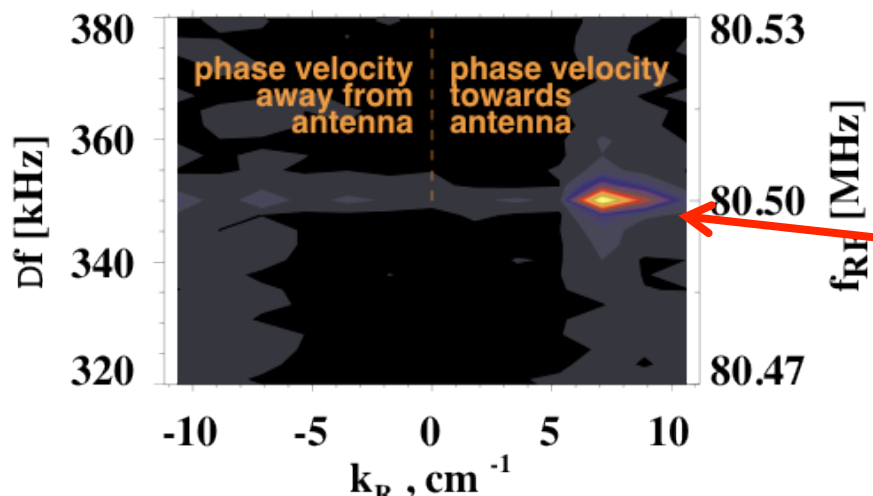
TORIC at  $240N_r \times 255 N_m$

- Both codes are using the same equilibrium from an Alcator C-Mod discharge with mixture of D- $^3\text{He}$ -H in (21%-23%-33%) of  $n_e$  proportion.
- ICW previously predicted by F.W. Perkins Nuclear Fusion 17 (1977)1197

AORSA at  $230N_x \times 230 N_y$

# The mode converted ICW was observed in Alcator C-Mod using the PCI diagnostic

Contour Plot of Fourier Analyzed PCI Data

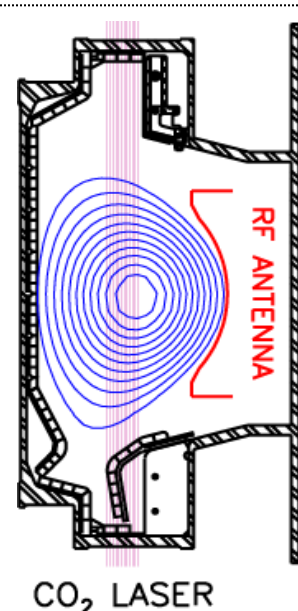


Most sensitive to waves with vertically aligned wave fronts.

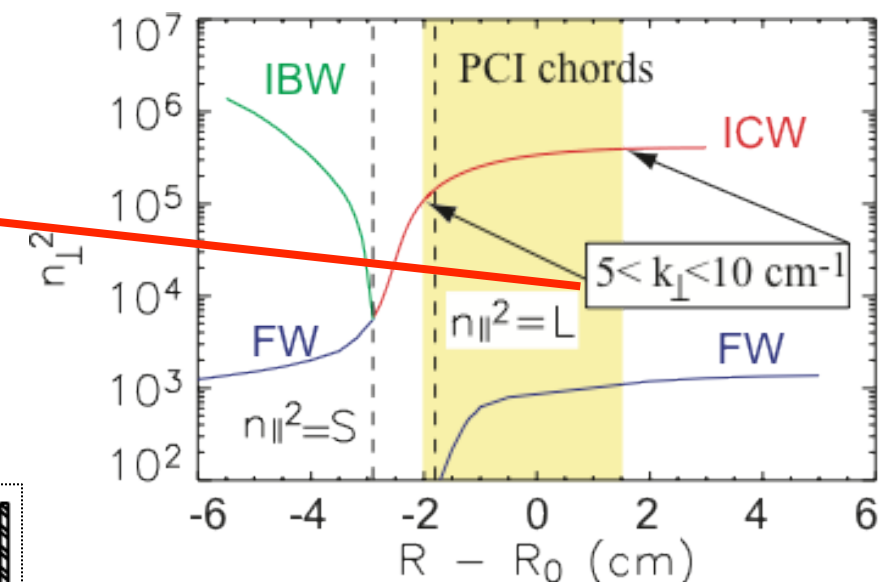
$\text{CO}_2$  Laser intensity modulated  $\rightarrow$  rf signals detected at beat frequency.

Wave  $k_R$  obtained by Fourier transformation on signals from all 12 channels.

A. Mazurenko, PhD thesis, MIT(2001).



Dispersion Curves near MC Region

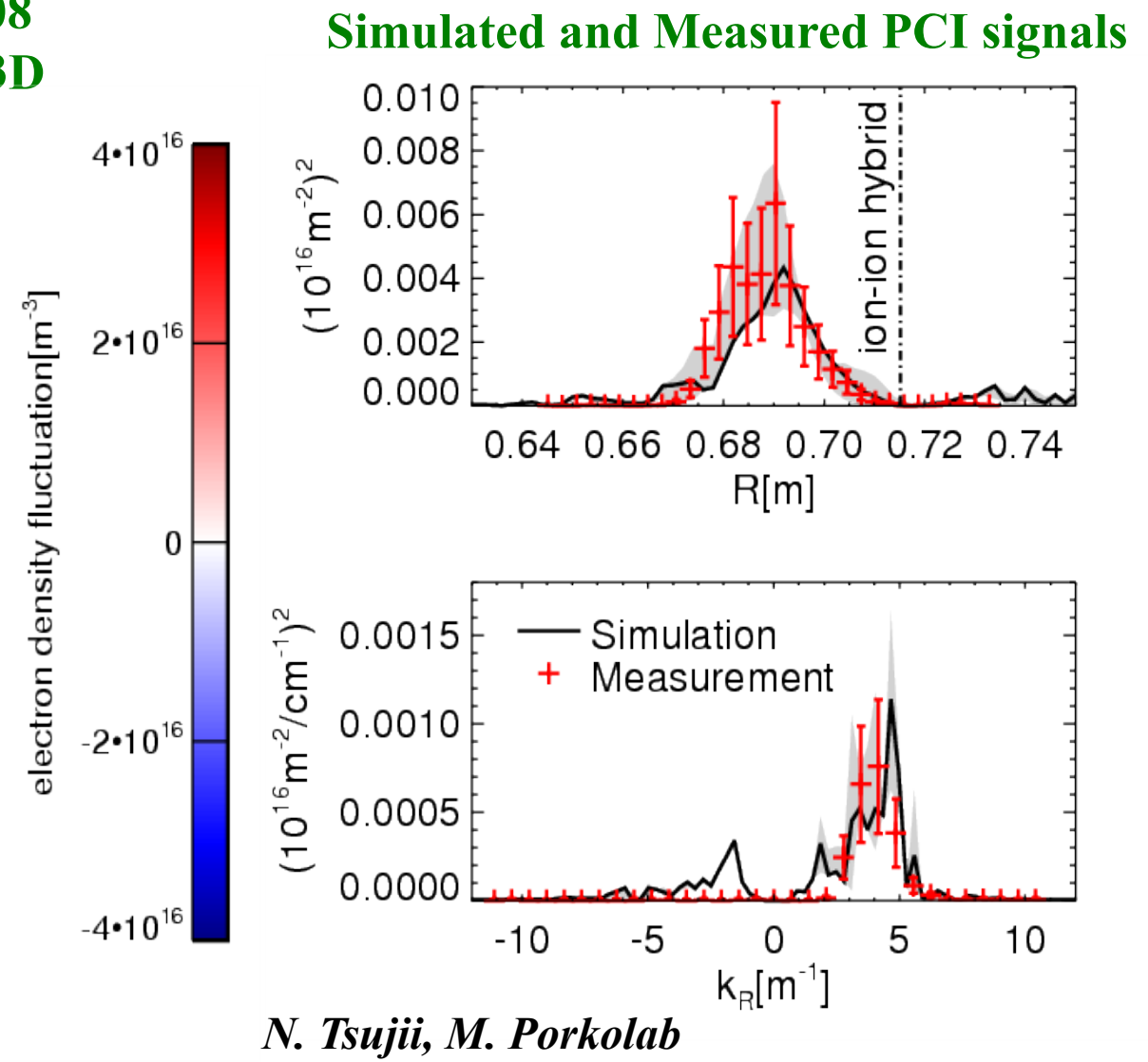
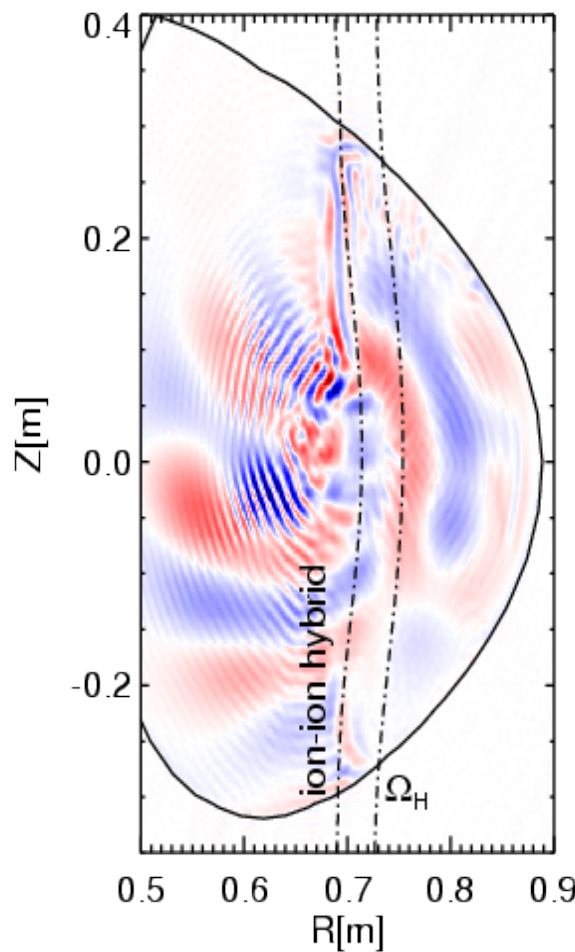


- Propagating towards the low field side.
- Wavelength shorter than FW, but generally longer than IBW.
- On the low field side of the  $\text{H}-\text{He}^3$  hybrid layer.

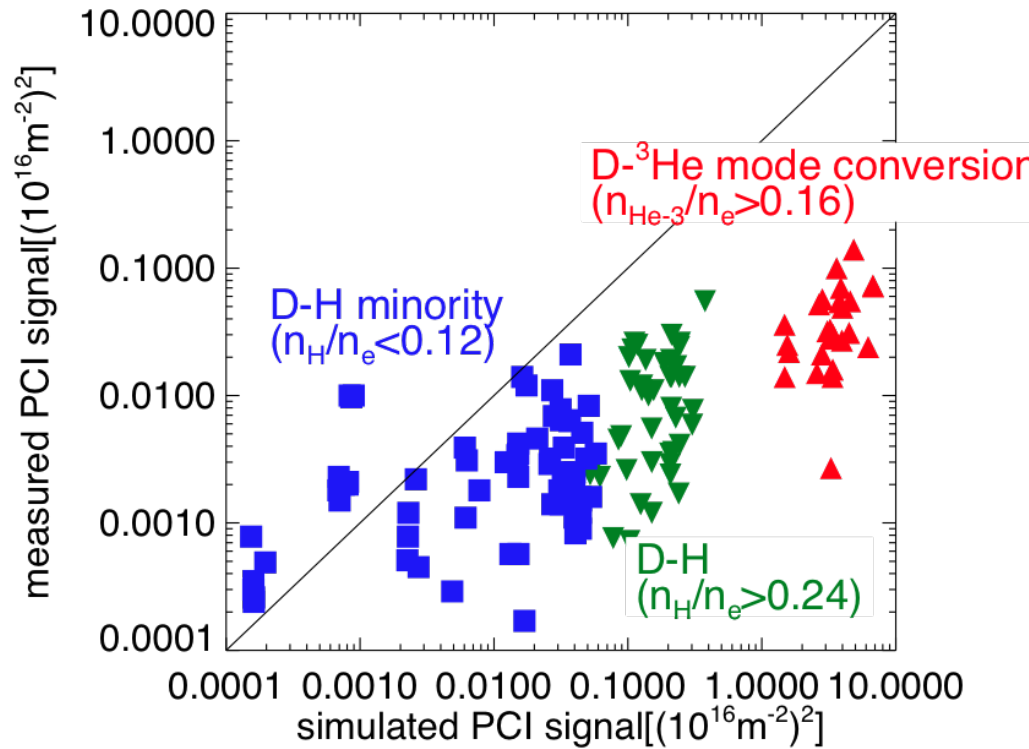
E. Nelson-Melby *et al*, PRL 90 (15) 155004 (2003)

# Fluctuation measurement with PCI consistent with 3-D ICRF full-wave simulations in strong damping regime

D(H) plasma,  $n_H/n_e = 0.08$   
Simulation: AORSA+CQL3D



# Recent detailed comparison of measured and simulated PCI signals find significant quantitative differences



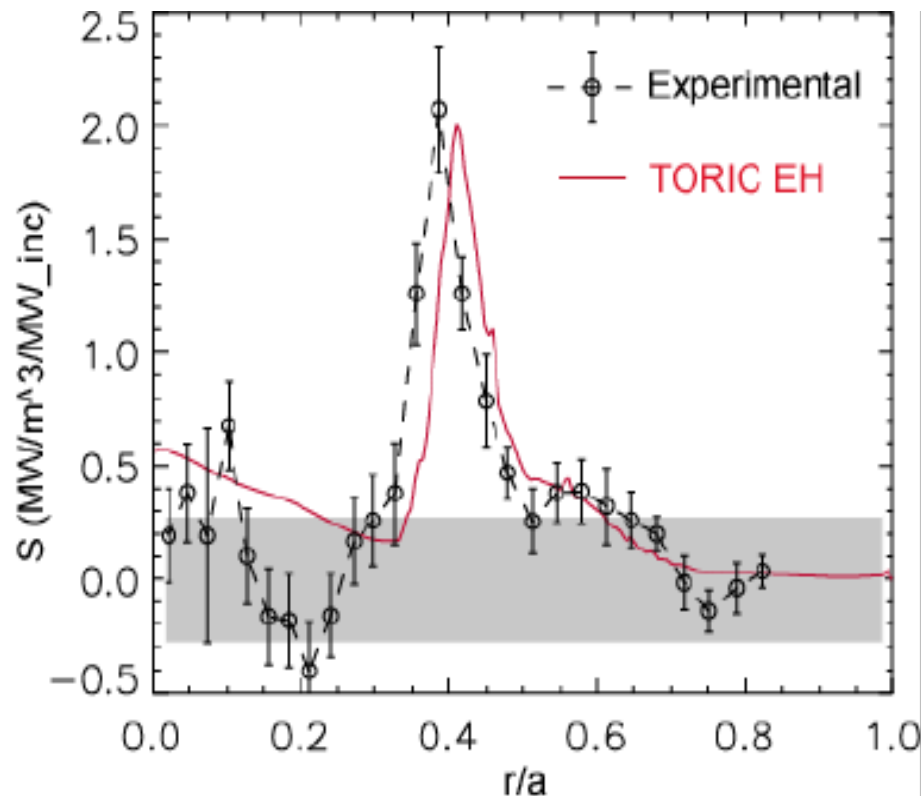
N. Tsujii, M. Porkolab et al  
Paper in preparation

3D AORSA – CQL3D  
simulations  
~10<sup>5</sup> cpu-hours on NERSC  
per point on this figure

*Reason for disagreement is not understood, particularly since the observed electron damping is strong:*

*neglect of nonlinear effects? diagnostic difficulty? Error in synthetic diagnostic? Other damping mechanisms?*

# Simulations do agree with measurements of electron absorption in off-axis mode conversion in C-Mod\*



$f_{\text{rf}} = 80 \text{ MHz}, 22.5\% \text{H}, 77.5\% \text{D}$   
 $B_t = 5.27 \text{ T}, I_p = 1 \text{ MA},$   
 $n_e = 1.8 \times 10^{20} \text{ m}^{-3}, T_e = 1.8 \text{ keV}$   
 $t = 1.502 \text{ sec, E antenna}$

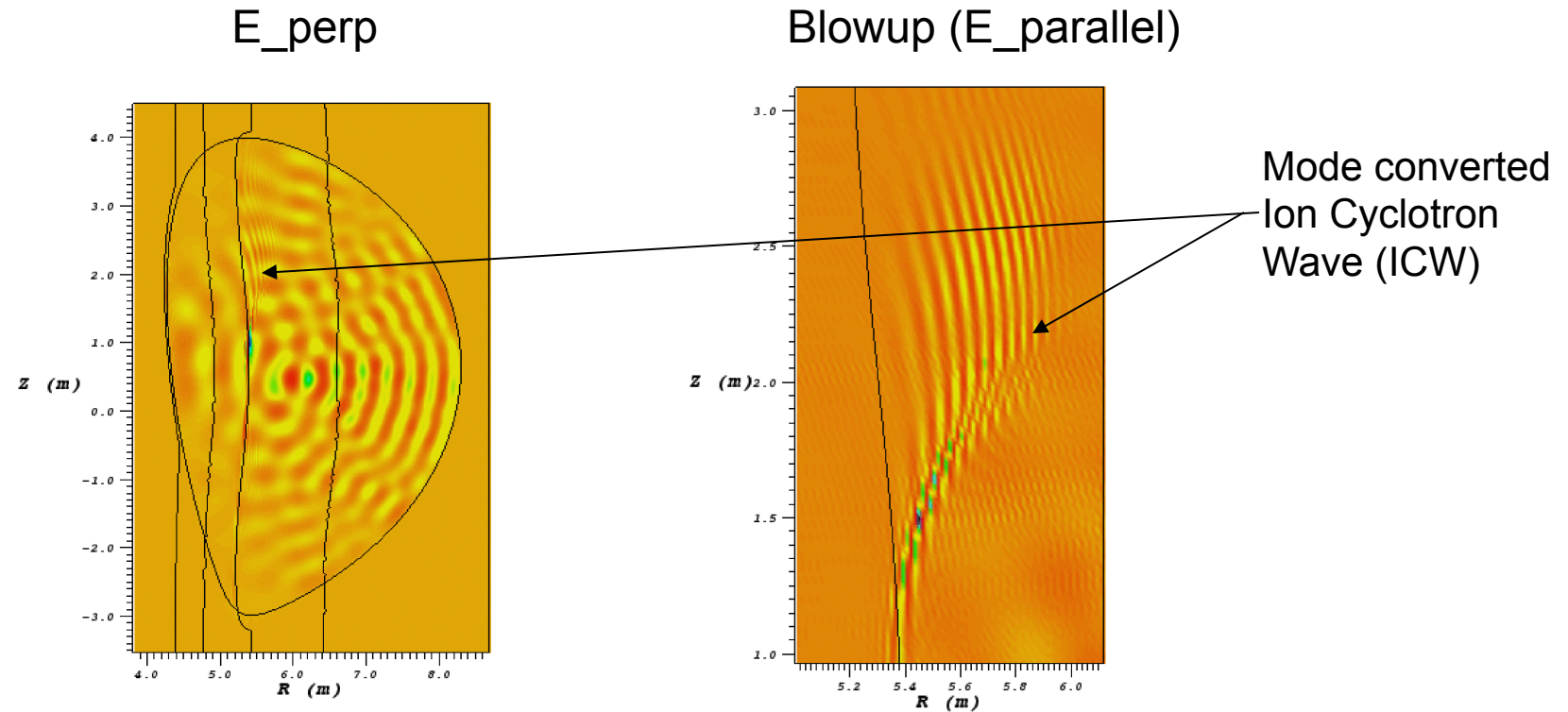
- Off-axis MC
  - D-H hybrid layer at  $r/a = 0.35$  (HFS)
- Good agreement of experiment curve and TORIC.
- Total  $\eta^{\text{MCEH}}$  in the MC region ( $0.35 < r/a < 0.7$ )
  - Experiment: 20%
  - TORIC: 18%
- TORIC is now used routinely by C-Mod experimentalists to analyze ICRF heated discharges.

Similar agreement found with on-axis mode conversion experiments

\*[Y. Lin *et al*, 15th Top. Conf. On RF Power in Plasmas, 2003]

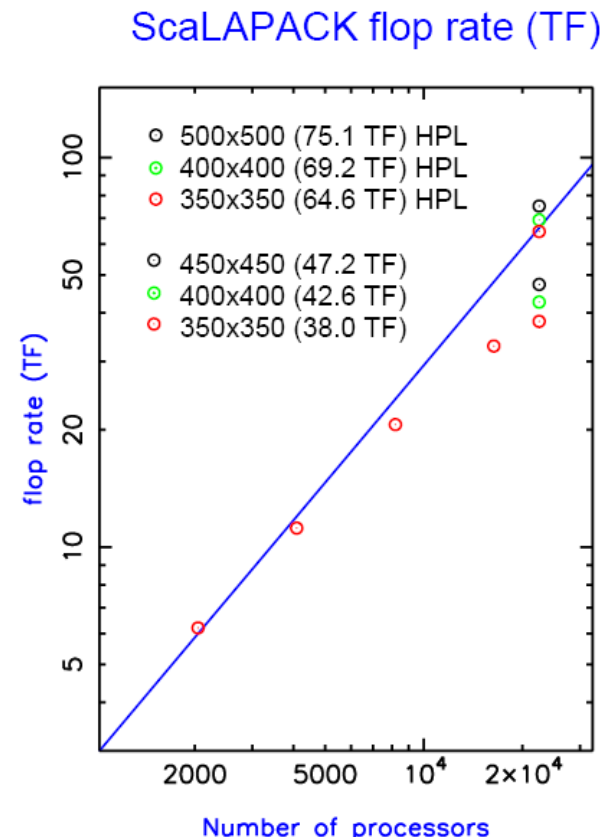
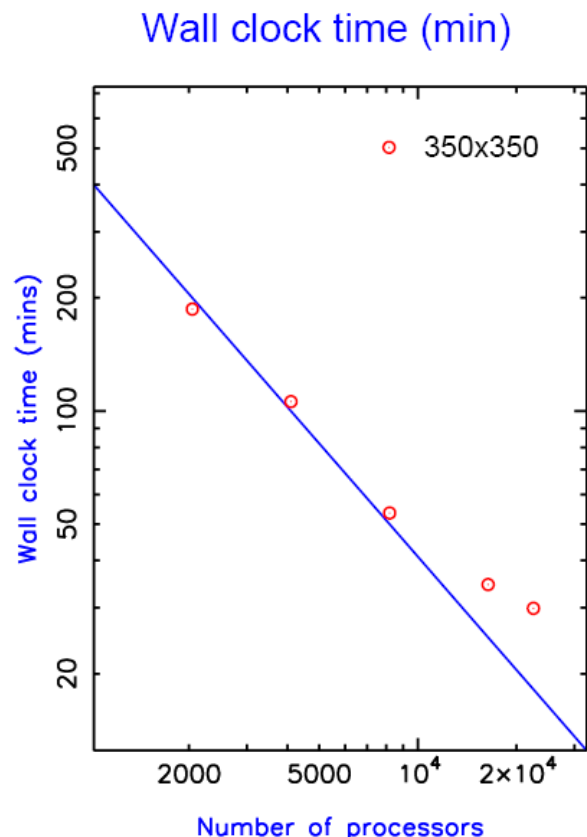
# Calculations on the Cray XT3 have allowed the first simulations of mode conversion in ITER

ITER with D:T: $^3\text{He}$  = 20:20:30 with  $N_R = N_Z = 350$ ,  $f = 53 \text{ MHz}$ ,  $n = 2.5 \times 10^{19} \text{ m}^{-3}$   
[4096 processors for 1.5 hours on Jaquar (Cray XT-3)]

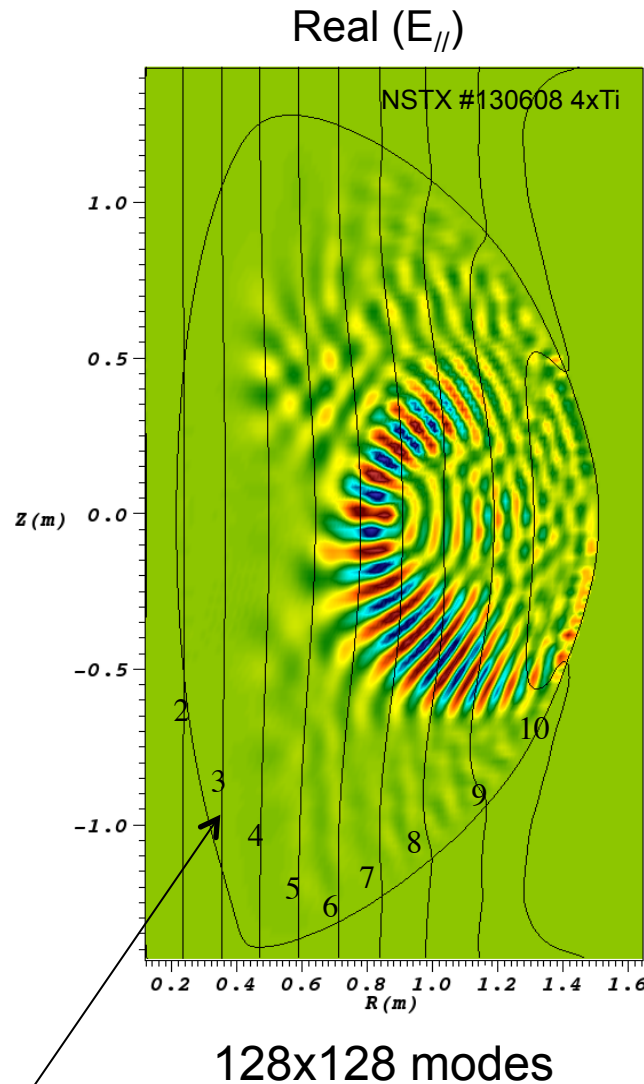


# Scaling of Full-wave ICRF solvers to > 20,000 processors demonstrated for ICW Mode Conversion in ITER

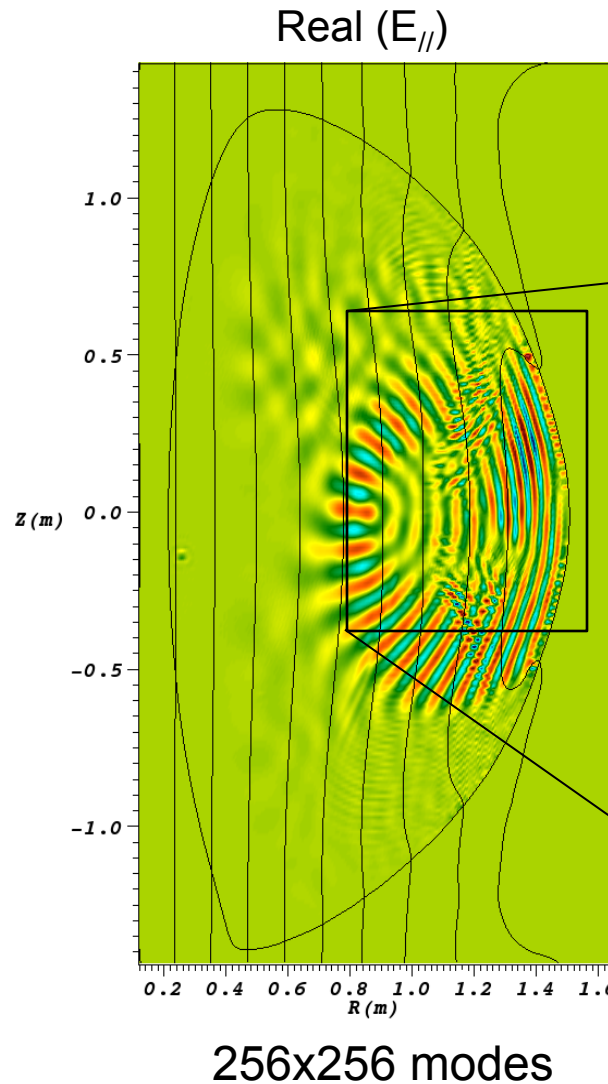
ITER with D:T:HE3 = 20:20:30 with  $N_R = N_Z = 500$ ,  $f = 53$  MHz,  $n = 2.5 \times 10^{19} \text{ m}^{-3}$



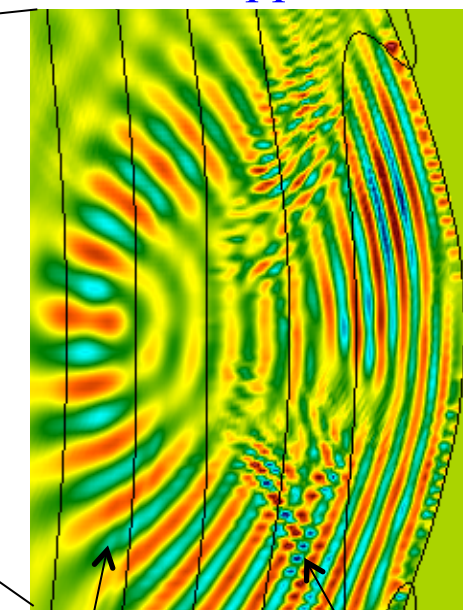
# A new wave appears as the spatial resolution is refined in NSTX High Harmonic Fast Wave Experiments



D ion cyclotron layers



AORSA:  
~20 min with 2304  
processors on  
Hopper



HHFW

new  
mode

*Seen in both AORSA and TORIC simulations*

## Another slow wave can propagate if the electrons are “warm” with $\omega \ll k_{\parallel} v_{te}$

Assuming cold ions (neglects IBW) and warm electrons, the simplest wave dispersion relation can be written as:

$$a n_{\perp}^4 - b n_{\perp}^2 + c = 0$$

$$a = K_{xx,\text{cold}} = S = 1 - \sum_s \frac{\omega_{ps}^2}{\omega^2 - \Omega_{cs}^2}, \quad b = -K_{zz}(n_{\parallel}^2 - S),$$

where

$$c = K_{zz}(n_{\parallel}^2 - R)(n_{\parallel}^2 - L) \quad \text{where} \quad S = \frac{1}{2}(R + L)$$

“fast root”:  $n_{\perp}^2 \sim c / b \sim (n_{\parallel}^2 - R)(n_{\parallel}^2 - L) / (S - n_{\parallel}^2)$

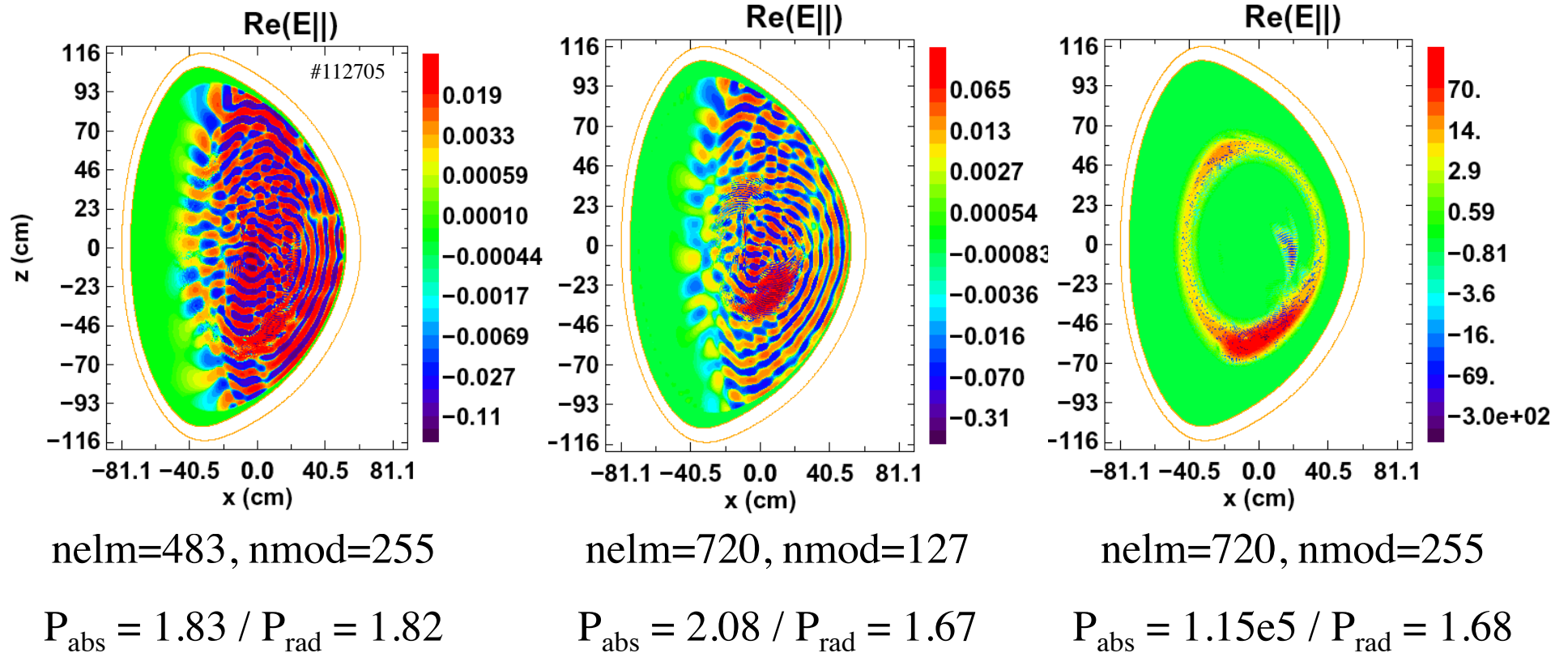
“slow root”:  $n_{\perp}^2 \sim b / a \sim -K_{zz} (n_{\parallel}^2 - S) / S$

>> The slow wave has been **assumed** to be evanescent, with  $K_{zz} \sim -\omega_{pe}^2 / \omega^2$  and  $S < 0$  for  $\Omega_i < \omega$  in the ICRF and HHFW regimes with low field side launch.

>> With “warm” electrons,  $K_{zz} \sim 2\omega_{pe}^2 / k_{\parallel}^2 v_{te}^2 > 0$  so the slow wave can propagate

**Slow wave appears as resolution is increased....  
but power balance eventually degrades**

TORIC HHFW code



*Similar difficulties occur with AORSA*

# Does the mode exist in experiments ..... or only in the simulations?

*New mode is consistent with simple theoretical model:*

- Requires  $B_p$  upshift of  $k_{\parallel}$  and finite  $T_e$  for “warm electron effects”
- Related to warm electrostatic ICW first observed by Motley and D’Angelo in a Q-machine (1961)
- Independent of  $T_i \rightarrow$  not an ion Bernstein wave
- Electron damping, kinetic flux and finite  $E_{\parallel}$  associated with mode
- Found in simulations of ICRF regime and in HHFW regime

*New mode seen with two independent full wave codes, but:*

- simulations do not converge at even finer grids – perhaps new mode is not yet fully resolved or another wave is also being excited?
- Predicted wavelengths differ from those found in the NSTX HHFW regime, but not in the C-Mod ICRF experiments – perhaps due to the higher shear in NSTX?

*Existing diagnostics in experiments not designed to detect mode (yet)*

*Harder Problem: RF-induced slow-time evolution of the equilibrium distribution functions must be included in the simulations*

- RF interactions cause a slow time-evolution of the velocity space dependence of the equilibrium plasma distribution functions (e.g., minority heating)
- Neutral beam injection which is used simultaneously with rf heating introduces energetic ions into the plasma that can resonantly interact with the rf
- In burning plasmas in ITER, the fusion reactions will produce energetic alpha particles that can interact with the rf waves  
*Methods used thus far are costly .....*  
*and it is difficult to include important physics effects*



# Quasilinear approximation includes rf-induced slow time evolution of the plasma equilibrium distributions

For time harmonic (rapidly oscillating) wave fields  $\mathbf{E}$  with frequency  $\omega$ , Maxwell's equations reduce to the Helmholtz wave equation:

$$-\nabla \times \nabla \times \mathbf{E} + \frac{\omega^2}{c^2} \left( \mathbf{E} + \frac{4\pi i}{\omega} \mathbf{J}_p \right) = -\frac{4\pi i \omega}{c^2} \mathbf{J}_{\text{ant}}$$

The plasma current ( $\mathbf{J}_p$ ) is a non-local, integral operator (and non-linear) on the rf electric field and conductivity kernel:

$$\mathbf{J}_p(\mathbf{r}, t) = \sum_s \int d\mathbf{r}' \int_{-\infty}^t dt' \sigma(f_{0,s}(E), \mathbf{r}, \mathbf{r}', t, t') \mathbf{E}(\mathbf{r}', t')$$

The long time scale response of the plasma distribution function is obtained from the bounce averaged Fokker-Planck equation or a Monte Carlo orbit code:

$$\frac{\partial}{\partial t} (\lambda f_0) = \nabla_{\mathbf{u}_0} \cdot \Gamma_{\mathbf{u}_0} + \langle\langle S \rangle\rangle + \langle\langle R \rangle\rangle^0 \quad \text{where} \quad \nabla_{\mathbf{u}} \cdot \Gamma_{\mathbf{u}} = C(f_0) + Q(\mathbf{E}, f_0)$$

**Wave Solvers**  
**(AORSA)**  
**(TORIC)**

**distribution**  
**function**  
**evolution**  
**(CQL3D or**  
**ORBIT-RF)**



*Need to solve this nonlinear, integral set of equations for wave fields and velocity distribution function self-consistently. This requires an iterative process to attain self-consistency.*

# Simple model can illustrate the rf-induced quasi-linear time evolution of the resonant zero<sup>th</sup> order particle distribution function

Consider unmagnetized 1D plasma:

$$\frac{\partial f}{\partial t} + v \frac{\partial f}{\partial z} + \frac{q}{m} E \frac{\partial f}{\partial v} = 0$$

Assume:  $f(z, v, t) = f_0(v, t) + f_1(z, v, t)$        $\vec{E} = \vec{E}_0 + \vec{E}_1 = \vec{E}_1$

where  $f_1(z, v, t) = \int_{-\infty}^{\infty} \frac{dk}{2\pi} f_k(k, v, t) e^{ikz}$  and  $E_1 = \int_{-\infty}^{\infty} \frac{dk}{2\pi} E_k e^{ikz}$

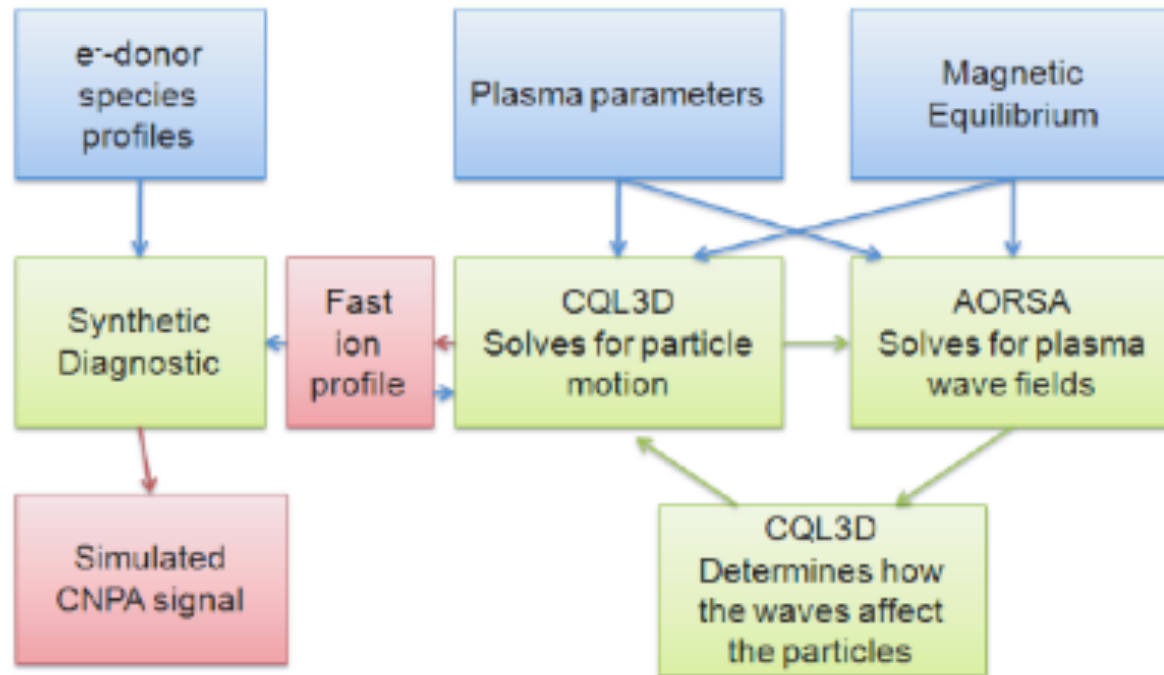
Define:  $\langle f \rangle = \lim_{L \rightarrow \infty} \frac{1}{L} \int_{-\infty}^{\infty} dx f$  with  $\langle f \rangle = f_0(v, t)$  and  $\langle E \rangle = 0$

Then:  $\frac{\partial}{\partial t} f_0(v, t) = -\frac{q}{m} \frac{\partial}{\partial v} \langle E f_1 \rangle \Rightarrow \frac{\partial}{\partial v} D \frac{\partial}{\partial v} f_0$

with  $D \sim (\dots) \int \frac{dk}{2\pi} \left\{ iP \left( \frac{E_k E_{-k}}{\omega - kv} \right) + \pi \delta(\omega - kv) E_k E_{-k} \right\}$

*Much more complicated in magnetized plasma  
see Kennel and Engelmann PF 9(1966)2377*

# Many cpu-hours are required to self-consistently solve the wave and the bounce-averaged Fokker-Planck equations



Inputs are blue  
Outputs are red

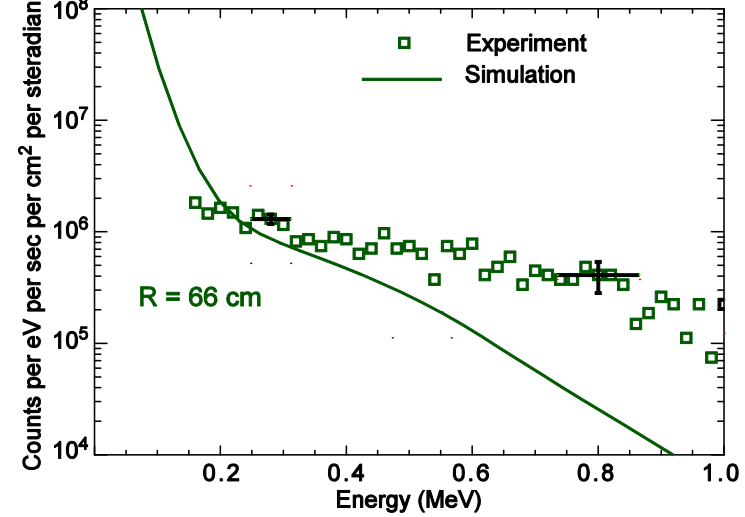
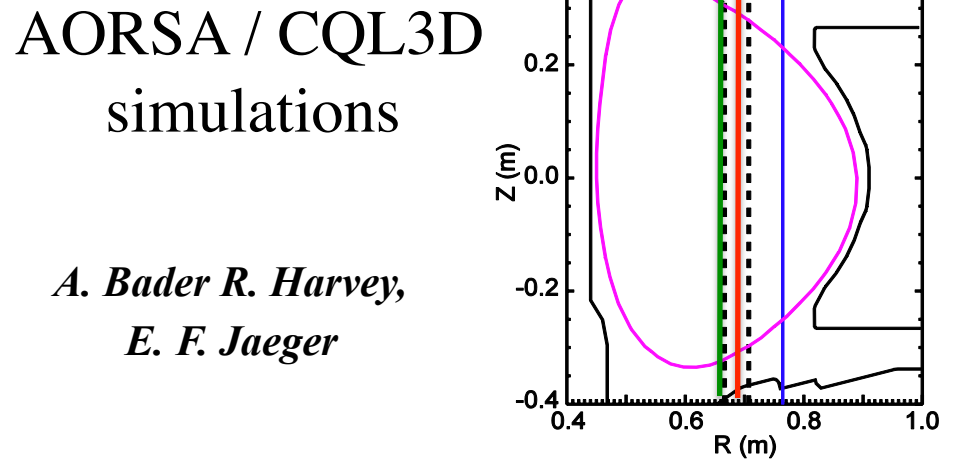
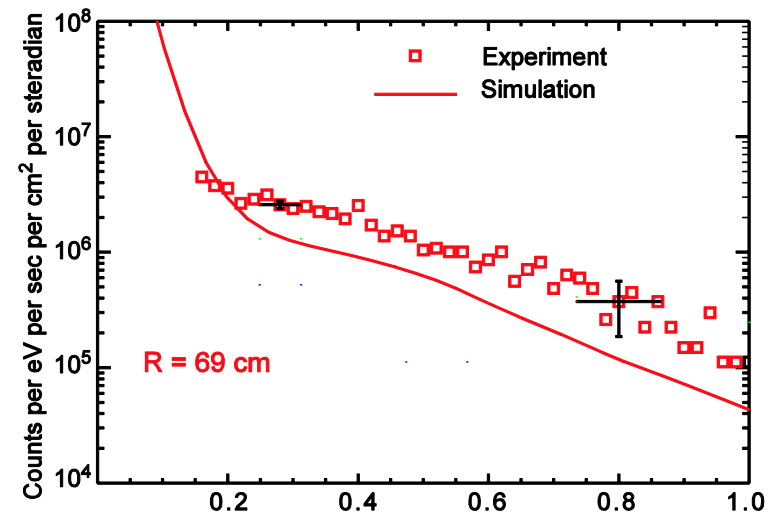
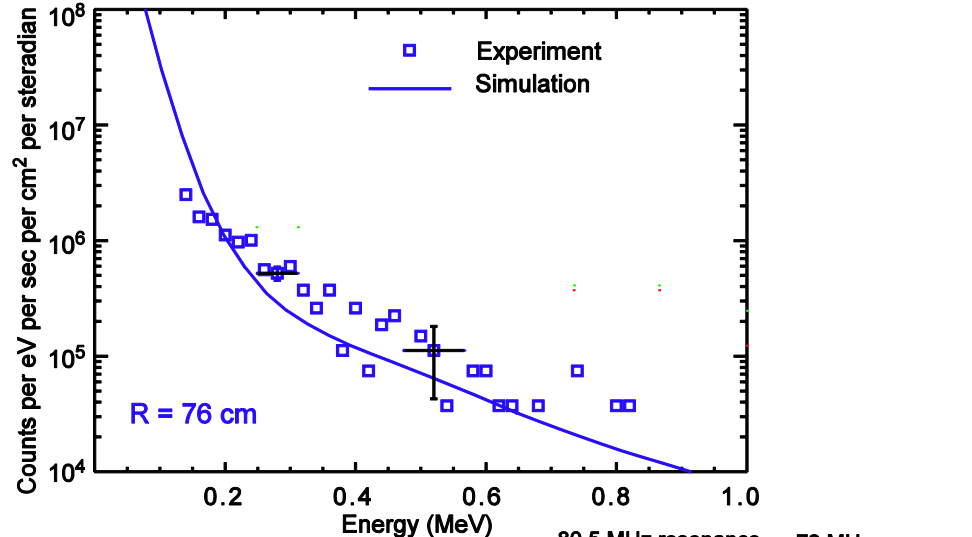
Iterate AORSA [wave solver] with CQL3D [bounce averaged, zero banana width, Fokker Planck code] to produce self-consistent fields, power deposition profiles, and resonant particle distribution function, and simulated diagnostic signals

For ICRF minority heating in C-Mod, typical requires ~3000 Cpu-hours

# Synthetic diagnostics have been developed to test predictive capability of combined ICRF full-wave & Fokker Planck solvers against specific diagnostic data

- **CNPA data** has been compared with synthetic diagnostic signal based on non-thermal ion tail from combined CQL3D / AORSA simulations of minority ICRF heating experiments on Alcator C- Mod:
  - *Results thus far properly simulate energy dependence and magnitude of CNPA spectra but point to possible importance of radial losses.*
  - *Future work will combine Monte Carlo codes sMC or ORBIT RF with AORSA/TORIC to assess finite orbit width effects.*
- **FIDA data** has been compared with synthetic diagnostic signal based on non-thermal ion tail from combined ORBIT RF / AORSA simulations of HHFW – fast ion interaction experiments in NSTX and DIII-D:
  - *Results thus far indicate that finite ion orbit width effects are important in order to reproduce the spatial profiles of experimentally measured FIDA.*

# Agreement of simulations of CNPA data degrades close to the ICRF resonance layer in minority heating on C-Mod

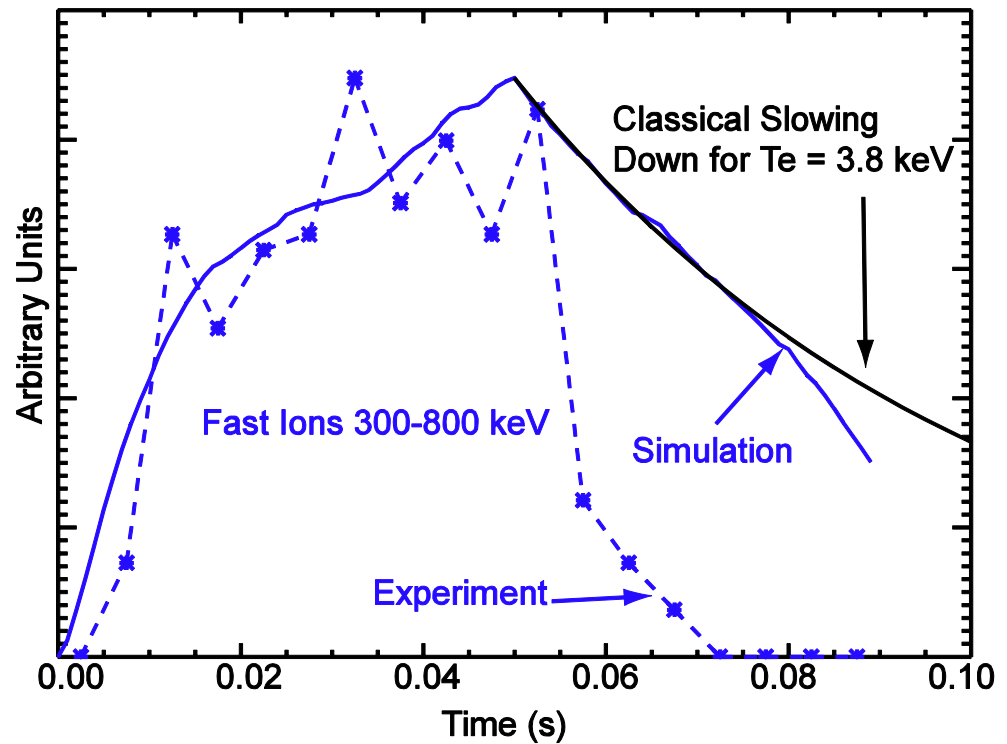


A. Bader R. Harvey,  
E. F. Jaeger

*QL theory may not apply ( $\Delta E_{fi} \approx E_f$ ) or finite ion orbit width effects may be important.*

# Time-dependent simulations $\Rightarrow$ reasonable agreement during rise, poor agreement during decay

- Time dependent simulations of a 50 ms on, 40 ms off ICRF signal.
- CQL3D was advanced in time using 1 ms time steps and calling AORSA after every ms, for the 50 ms turn-on time.
- Simulations included the background evolving plasma.
- Results find reasonable agreement during the turn-on time, but significant disagreement during the turn-off time.
- Discrepancy is similar across all energy bins.

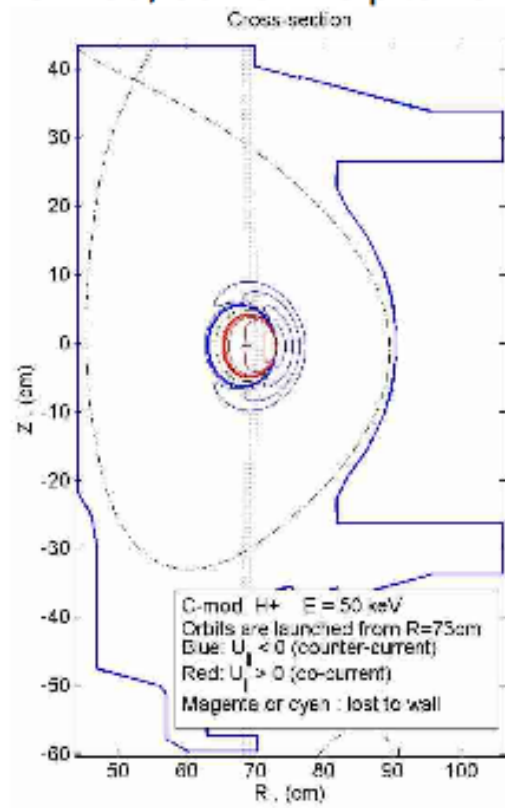


- Additional radial diffusion, with inverse dependence on particle energy, may account for the discrepancy.

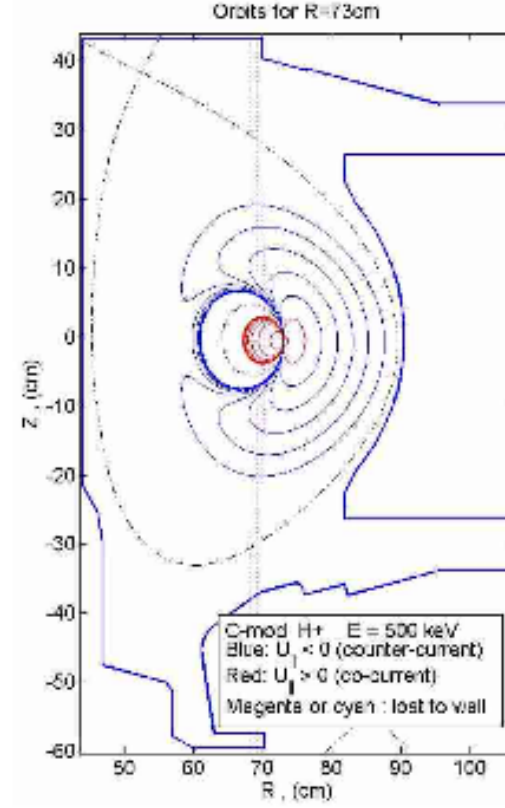
*A. Bader, R. Harvey, E. F. Jaeger*

# Full orbit topologies included in $D_{QL}$ by direct integration of Lorentz force equation in the combined equilibrium and rf wave fields from AORSA

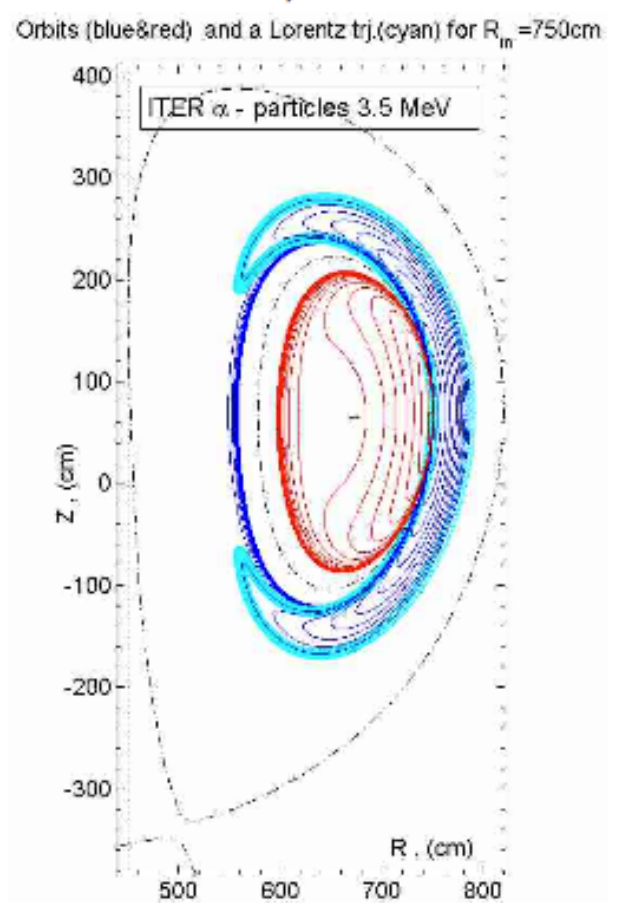
C-Mod, 50 keV vs pitch angle



C-Mode, 500 keV

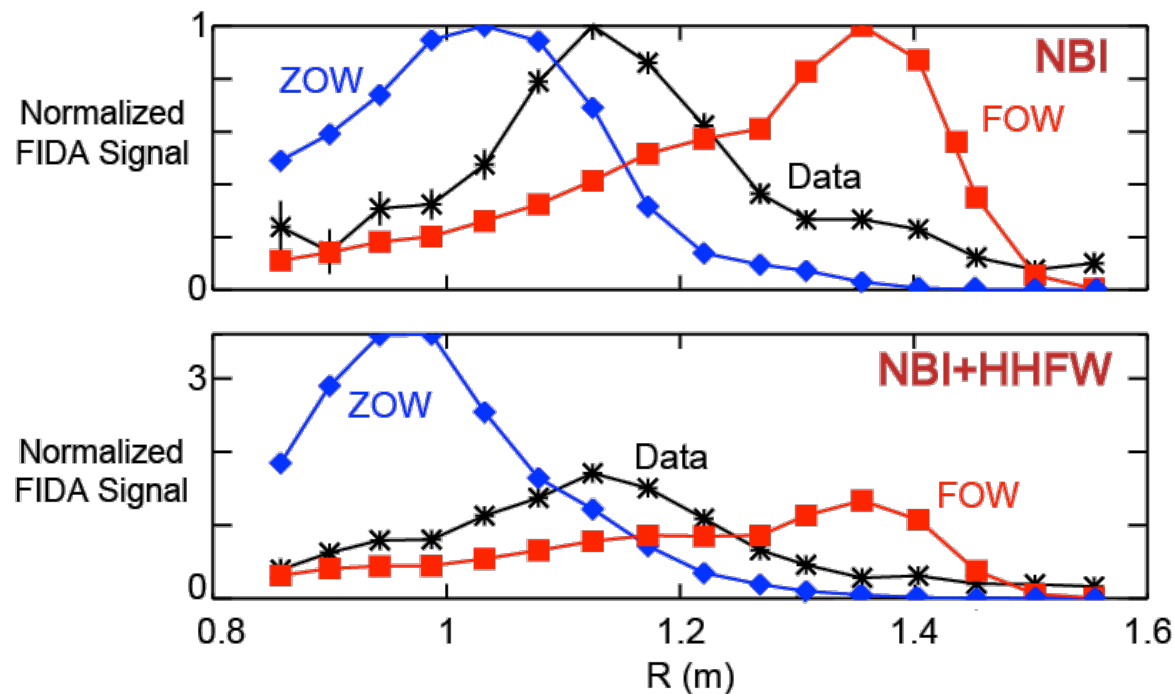


ITER, 3.5 MeV



The DC code constructs the bounce-averaged  $D_{QL}$  from the integrated orbits and uses it to iterate between AORSA and CQL3D

# Simulations of FIDA data on NSTX that finite orbit widths and fast ion losses need to be considered



Recent FIDA simulations using "hybrid" full-orbit FOW CQL3D show large outboard shift of simulated FIDA profile relative to ZOW model:

- "Hybrid" FOW CQL3D has full orbits but does not treat orbit topologies correctly at trapped-passing boundaries

- Expect that proper treatment of orbit topologies will bring the simulations into better agreement with FIDA data

A full-orbit neoclassical transport model, and losses to SOL and wall still needs to be implemented

Initial tests of full-orbit FOW CQL3D show accurate modeling of fast-ion losses and power absorption and RF-driven current profiles

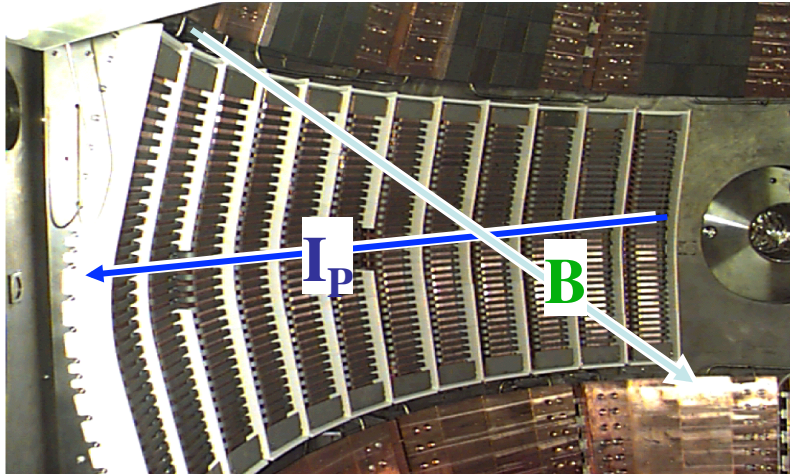
***Hardest Problem: Need to simulate RF fields from the magnetic axis all the way to the antenna and vessel wall to be able to predict RF effects on plasma performance in ITER and other devices***

- The equilibrium geometry is really 3D outside of the last closed flux surface, so additional fine-scale features in the wave fields are anticipated
- Wave interactions with the antenna can alter the spectrum of waves that are excited in the plasma, and can cause failures in the antenna (arcs, etc)
- Experimental data on edge rf fields and equilibrium profiles is scarce, and rf physics in the edge is not well understood
- Non-linear effect are known to be present (parametric decay instabilities, etc)

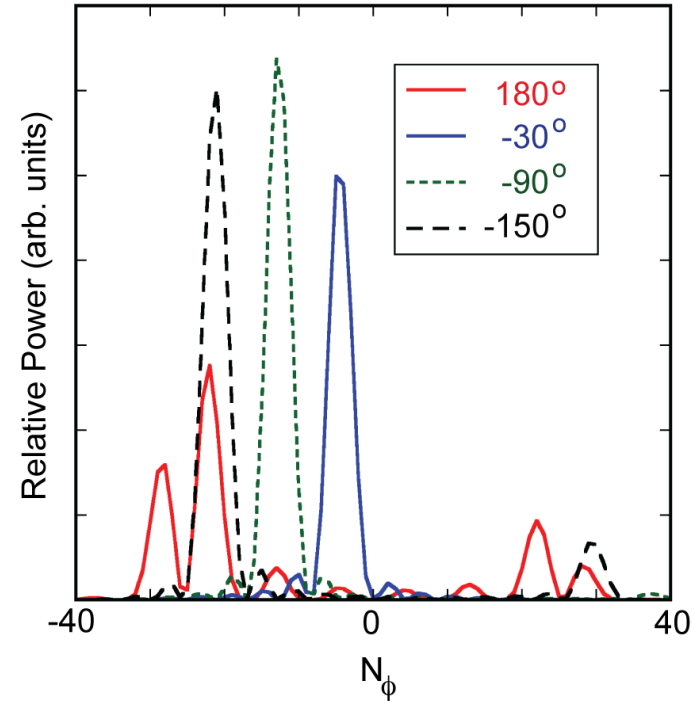
Only recently have basic core-to-edge simulations been attempted



# RF antennas as well as vacuum vessel, ports, etc introduce 3D structures outside of the LCFS

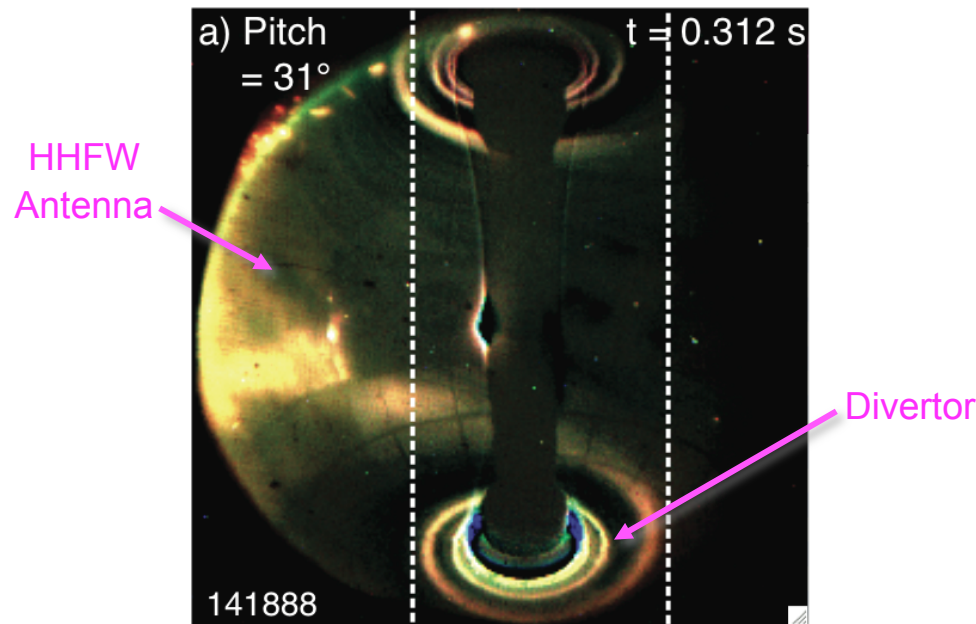


NSTX HIFW antenna extends toroidally  $90^\circ$



- Phase between adjacent straps easily adjusted between  $0^\circ$  to  $180^\circ$
- Large B pitch affects wave spectrum in plasma core

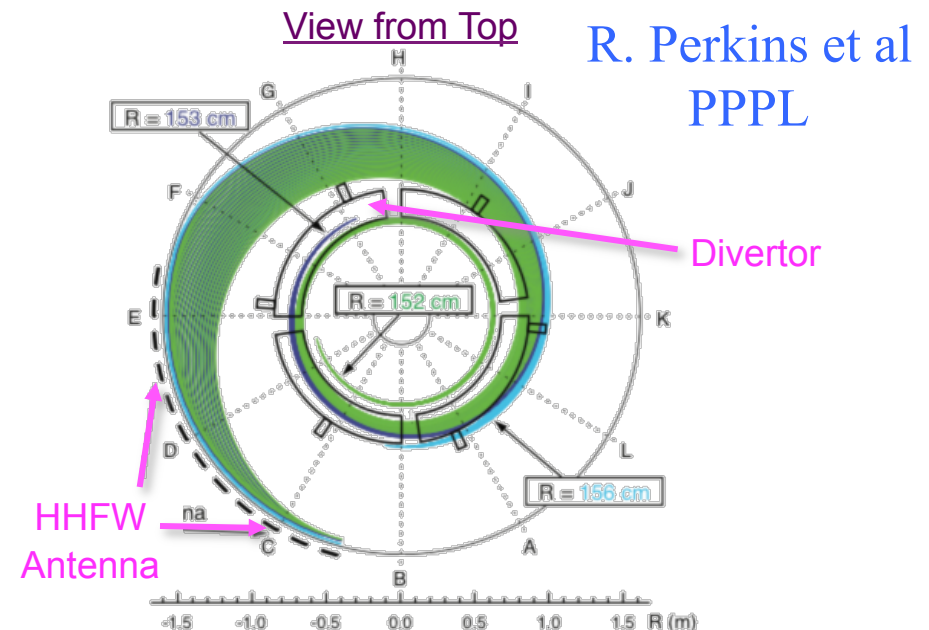
# Significant fraction of the HHFW power in NSTX may be lost in the plasma outside of the LCFS



Plasma TV image shows edge RF power deposition spiral flowing from HHFW antenna to the divertor region for edge field pitch = 31°

Field line mapping predicts RF power deposited in scrape off layer (SOL) or on the vessel structures, not antenna face

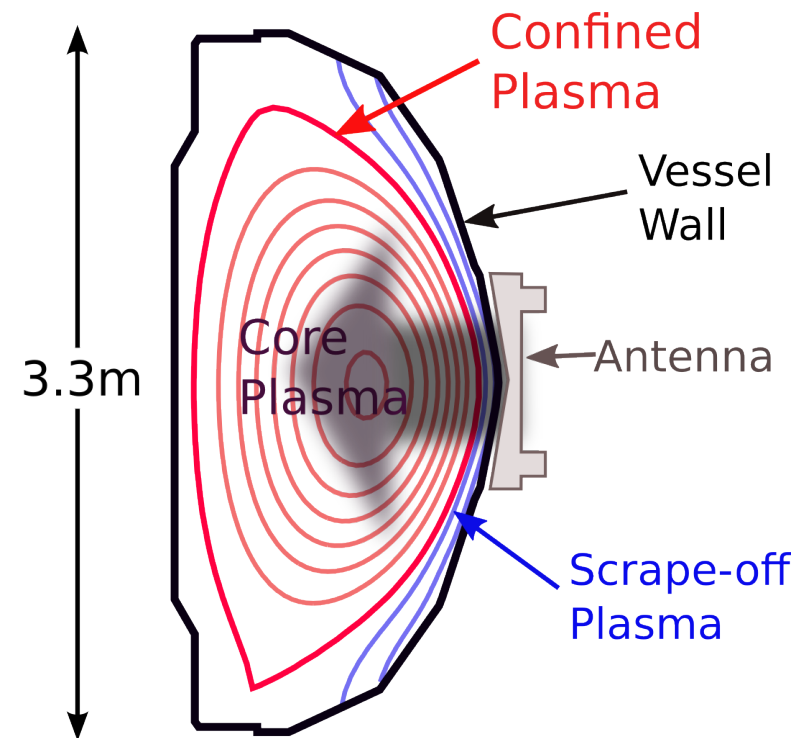
Indications exist for similar effects in other tokamaks  $\Rightarrow$  important for ITER



SPIRAL code results for edge field pitch = 31° show field lines (green) spiraling from the SOL in front of HHFW antenna to the lower divertor

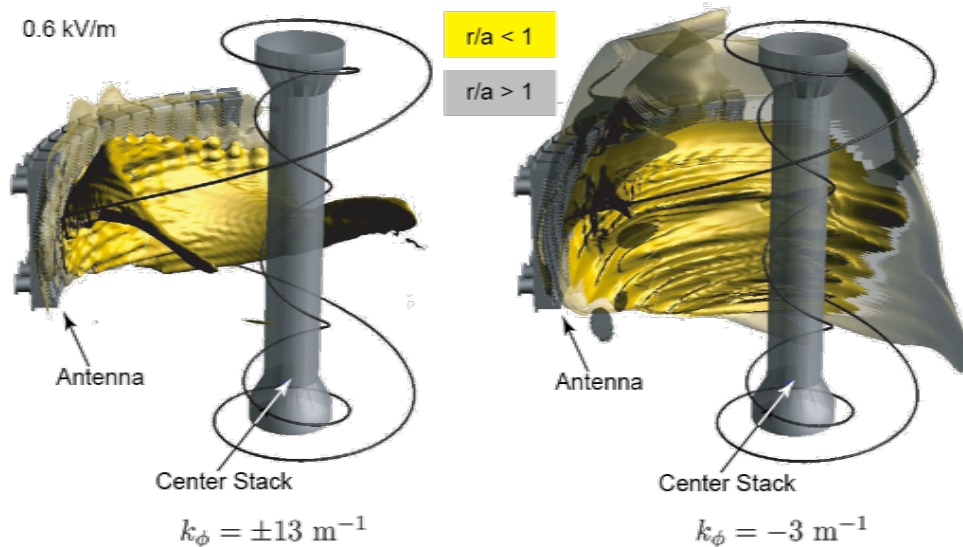
# AORSA has been extended to include the regions outside of the last closed flux surface

- AORSA contains a “mask” variable that controls which subset of the rectangular computational domain ( $R, Z$  mesh) are solved for.
  - Equivalent to enforcing zero electric field outside the mask.
- Traditional mask solves for inside  $\rho=1$  surface (LCFS)
- New mask solves for arbitrary 2D boundary, in general some modification to the “rlim/zlim” boundary from the g-eqdsk file.

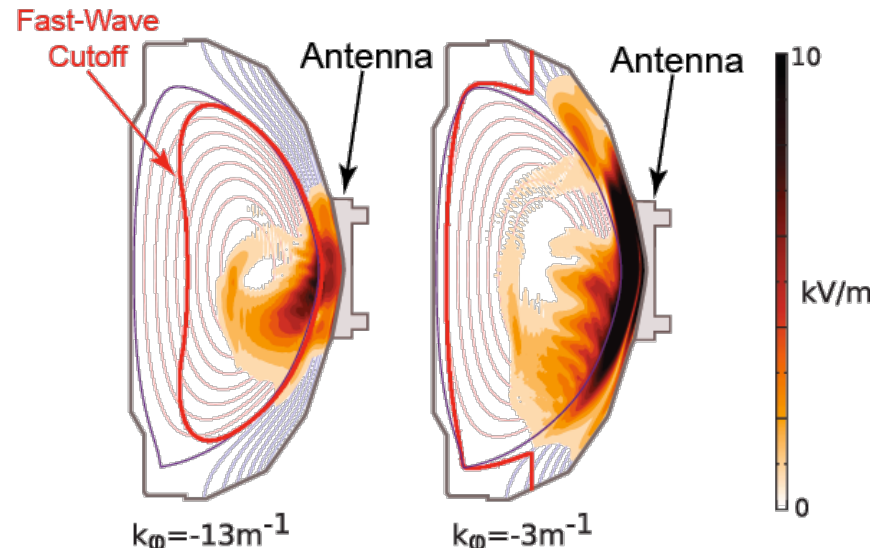


# AORSA predicts excitation of large amplitude coaxial standing modes between plasma and wall

Has implications for ITER ICRH, where the distance between the antenna/wall and the separatrix is large (0.1-0.2 m)



3-D AORSA simulation of NSTX shot 130608



2-D AORSA simulation of NSTX  
H-mode shot 130608

Quantitative comparison of predicted SOL electric fields with measurements underway:

- *Requires better resolution in the SOL & including geometry of the antenna & Faraday shield*

## *Exploring the Frontier:*

→ Adaptive Finite Elements and/or Wavelets – may provide a path to include edge region and true 3D equilibria

Time domain solutions – may provide a path to including nonlinear interactions in the edge and with the antenna

D.N. Smithe and T. Austin, TechX

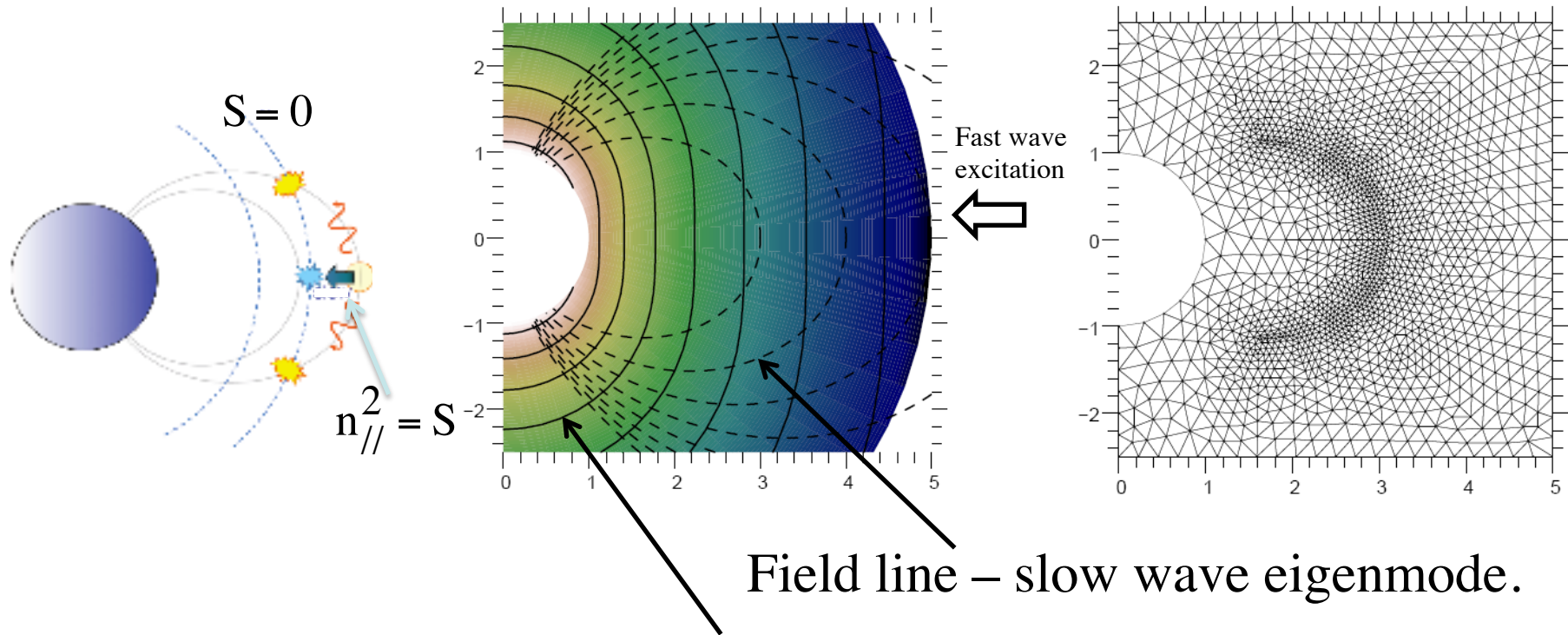
Particle in cell approaches – may provide a path to including antenna and edge interactions, as well as nonlinear effects

D.N. Smithe and T. Austin, TechX

## Adaptive FEM algorithms using unstructured meshes are being explored for modeling rf waves in the magnetosphere as well as rf heating outside of the LCFS

- Readily adapted to complex boundaries
- Readily refined as needed, in the vicinity of singular surfaces
  - For the magnetospheric problems under consideration, the multiple singular surfaces (mode conversion and resonance) do not simultaneously align with a structured mesh
- Mesh generation routines are readily available. (We use NAG)
- Readily applicable to cold plasma models (dielectric tensor is independent of  $k$ )
- Might be able to model 3D equilibrium effects in the edge regions
- *Big question: can hot plasma effects be included? (so that one core-to-edge code could be constructed?)*

## 2D effects are important in mode conversion from fast to slow waves in the earth's magnetosphere



$|B| = \text{const}$  -- cyclotron, ion-ion hybrid resonances

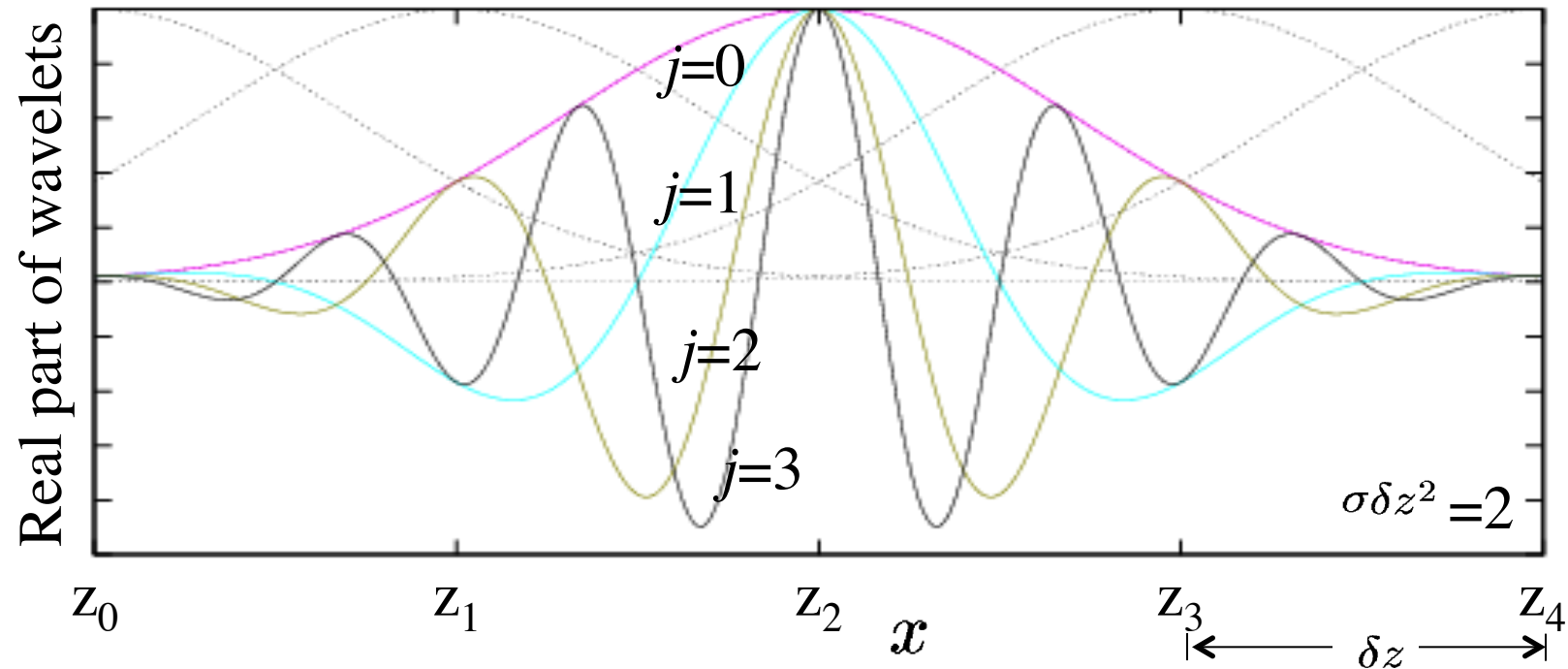
- an adaptive finite element code with an unstructured mesh has been developed and is being tested
- It will be adapted to model linear rf heating in the edge regions of fusion devices

# Wavelets may provide a more efficient expansion basis for the rf fields

Using a Gaussian envelope, Gabor wavelets localize a sinusoidal function

Gabor expansion:  $y(x) = \sum_{j,l} y_{(j,l)} e^{i k_j x} \exp\left(\frac{\sigma_j(x - z_l)^2}{2}\right)$  D.N. Smithe at al

Multiple envelopes with multiple harmonics in each



Dielectric tensor is similar to the Fourier-basis form but the velocity space integrals are much more complicated (e.g., some involve a logarithmic singularity) and the arguments of the Bessel functions are complex

# What are some of the major challenges in developing an accurate predictive simulation capability for rf heating in magnetized plasma?

- *Are there better methods than the commonly used, and reasonably successful, “spectral expansions” in full wave solvers?*
- *What is the best approach for core-to-edge simulations of the rf fields?*
  - *One wave code that covers the entire region? Or specialized regional codes that then must be linked together seamlessly?*
  - *Can time-domain or PIC codes be developed that can provide detailed simulations of linear and nonlinear wave-plasma interactions in the region outside of the last closed flux surface?*
  - *Can PIC simulations in the edge be matched to full wave solutions in the core?*
- *Can PIC or time-domain codes simulate wave-plasma interactions throughout the entire plasma?*
- *Are there techniques for improving the iterations between the full wave and QL solvers to simulate rf heating and its effects on the evolution of the plasma equilibria?*